

NAVAL POSTGRADUATE SCHOOL

Monterey, California



THESIS

DESIGN AND CONSTRUCTION OF A
MEDIUM RESOLVING, POWER SCANNING,
GRATING SPECTROMETER

by

James E. Hassett

December 1999

Thesis Advisor:
Co-Advisor:

D. Scott Davis
Andres Larraza

Approved for public release; distribution is unlimited.

20000310 037

REPORT DOCUMENTATION PAGE

Form Approved
OMB No. 0704-0188

Public reporting burden for this collection of information is estimated to average 1 hour per response, including the time for reviewing instruction, searching existing data sources, gathering and maintaining the data needed, and completing and reviewing the collection of information. Send comments regarding this burden estimate or any other aspect of this collection of information, including suggestions for reducing this burden, to Washington Headquarters Services, Directorate for Information Operations and Reports, 1215 Jefferson Davis Highway, Suite 1204, Arlington, VA 22202-4302, and to the Office of Management and Budget, Paperwork Reduction Project (0704-0188) Washington DC 20503.

1. AGENCY USE ONLY (Leave blank)	2. REPORT DATE December 1999	3. REPORT TYPE AND DATES COVERED Master's Thesis	
4. TITLE AND SUBTITLE DESIGN AND CONSTRUCTION OF A MEDIUM RESOLVING, POWER SCANNING, GRATING SPECTROMETER			5. FUNDING NUMBERS
6. AUTHOR(S) Hassett, James			8. PERFORMING ORGANIZATION REPORT NUMBER
7. PERFORMING ORGANIZATION NAME(S) AND ADDRESS(ES) Naval Postgraduate School Monterey, CA 93943-5000			
9. SPONSORING / MONITORING AGENCY NAME(S) AND ADDRESS(ES) N/A			10. SPONSORING / MONITORING AGENCY REPORT NUMBER
11. SUPPLEMENTARY NOTES The views expressed in this thesis are those of the author and do not reflect the official policy or position of the Department of Defense or the U.S. Government.			
12a. DISTRIBUTION / AVAILABILITY STATEMENT Approved for public release; distribution is unlimited.		12b. DISTRIBUTION CODE: A	
13. ABSTRACT (maximum 200 words) A scanning Ebert-Fastie spectrometer was designed and built for the Optical Physics and Sensors Laboratory of the Naval Postgraduate School. Optical design was done with two commercially available optical design software packages, OSLO LT by Sinclair Optics, Inc., and Optica by Wolfram Research, Inc. Several components for the spectrometer were designed and built at the Naval Postgraduate School Physics Department machine shop to include grating mount, motor mount, entrance and exit slits, gearbox, and spacers. Electronic interfaces included the motor, motor controller, and personal computer to control the diffraction grating angle, and a detector, data logger, lock-in detection system, and personal computer to record data. Data was measured from a Fe hollow cathode source to demonstrate proper operation. The recorded spectral lines were graphed in Microsoft Excel and tentatively identified as those tabulated in the published literature. Future work includes optimization of the resolving power and of the fore optics. Upon completion, the spectrometer will prove to be a very useful instructional aid in the optics and optoelectronics classes taught at the school, and as a medium resolving power visible and near ultraviolet instrument for future student thesis research.			
14. SUBJECT TERMS Spectrometer, Ebert-Fastie, Optics, Detector			15. NUMBER OF PAGES 90
			16. PRICE CODE
17. SECURITY CLASSIFICATION OF REPORT Unclassified	18. SECURITY CLASSIFICATION OF THIS PAGE Unclassified	19. SECURITY CLASSIFICATION OF ABSTRACT Unclassified	20. LIMITATION OF ABSTRACT UL

THIS PAGE INTENTIONALLY LEFT BLANK

Approved for public release; distribution is unlimited

**DESIGN AND CONSTRUCTION OF MEDIUM RESOLVING,
POWER SCANNING, GRATING SPECTROMETER**

James E. Hassett
Lieutenant Commander, United States Navy
B.S., Rensselaer Polytechnic Institute, 1989

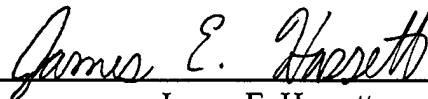
Submitted in partial fulfillment of the
requirements for the degree of

**MASTER OF SCIENCE IN APPLIED PHYSICS
AND
MASTER OF SCIENCE IN PHYSICS**

from the

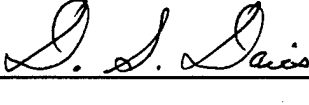
**NAVAL POSTGRADUATE SCHOOL
December 1999**

Author:

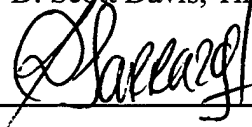


James E. Hassett

Approved by:



D. Scott Davis, Thesis Advisor



Andres Larraza, Co-Advisor



William B. Maier II, Chairman
Department of Physics

THIS PAGE INTENTIONALLY LEFT BLANK

ABSTRACT

A scanning Ebert-Fastie spectrometer was designed and built for the Optical Physics and Sensors Laboratory of the Naval Postgraduate School. Optical design was done with two commercially available optical design software packages, OSLO LT by Sinclair Optics, Inc., and Optica by Wolfram Research, Inc. Several components for the spectrometer were designed and built at the Naval Postgraduate School Physics Department machine shop to include grating mount, motor mount, entrance and exit slits, gearbox, and spacers. Electronic interfaces included the motor, motor controller, and personal computer to control the diffraction grating angle, and a detector, data logger, lock-in detection system, and personal computer to record data. Data was measured from a Fe hollow cathode source to demonstrate proper operation. The recorded spectral lines were graphed in Microsoft Excel and tentatively identified as those tabulated in the published literature. Future work includes optimization of the resolving power and of the fore optics. Upon completion, the spectrometer will prove to be a very useful instructional aid in the optics and optoelectronics classes taught at the school, and as a medium resolving power visible and near ultraviolet instrument for future student thesis research.

THIS PAGE INTENTIONALLY LEFT BLANK

TABLE OF CONTENTS

I.	INTRODUCTION	1
II.	BACKGROUND	3
	A. SPECTROMETER BASICS	3
	B. DIFFRACTION GRATING	4
	C. BLAZED DIFFRACTION GRATING	8
III.	OPTICAL DESIGN	11
	A. BASIC DESIGN CONSIDERATION.....	11
	B. CONSTRAINTS.....	12
	1. Diffraction Grating	12
	2. Available Commercial Optics.....	13
	3. Space Constraints.....	13
	C. OPTICAL DESIGN.....	14
	D. OPTICAL DESIGN SOFTWARE	16
IV.	MECHANICAL DESIGN	21
	A. OPTICAL MOUNTS.....	21
	B. SPACERS	22
	C. ROTATOR PLATE	24
	D. ENTRANCE AND EXIT SLITS.....	25
	E. MOTOR AND GEARBOX	26
	F. ASSEMBLY	29
V.	SPECTROMETER ALIGNMENT	31
	A. ALIGNMENT OF THE DIFFRACTION GRATING.....	31
	B. ALIGNMENT OF MIRRORS.....	32
	C. POSITIONING OF SLITS	35
VI.	SPECTROMETER CONTROL AND DATA ACQUISITION SYSTEMS	37
	A. MOTOR AND MOTOR CONTROLLER.....	37
	B. LIGHT SOURCE.....	38
	C. DETECTION SYSTEM	39
	1. Detector.....	39
	2. Lock-in Detection	40

3. Data Logger	42
VII. VERIFICATION OF OPERATION AND DATA ACQUISITION	45
A. DETERMINING GRATING ANGLE	45
B. SPECTROMETER OPERATION.....	47
C. REPRESENTATIVE SPECTROMETER DATA	48
VIII. CONCLUSIONS.....	51
APPENDIX A. DRAWINGS	53
APPENDIX B. MOTOR CONTROL COMPUTER PROGRAM.....	69
APPENDIX C. TABLE OF TENTATIVE IRON LINE IDENTIFICATIONS	73
LIST OF REFERENCES	77
INITIAL DISTRIBUTION LIST	79

ACKNOWLEDGMENT

The author would like to thank the following people for their support and contributions to this thesis project: Don Snyder for help in obtaining a computer, motor, and motor controller, and for the one-on-one instruction on the several softwares available to interface the motor to the computer; Gary Beck of the Physics Department Machine Shop for the precise and expedient construction of several mechanical components for the spectrometer; Professors Davis and Larraza for the many hours of help and instruction; and my wife Tammy for her incredible patience and encouragement during this rather long and painful process of writing this thesis.

THIS PAGE INTENTIONALLY LEFT BLANK

I. INTRODUCTION

I designed and built a scanning Ebert-Fastie spectrometer for the Optical Physics and Sensors Laboratory of the Department of Physics at the Naval Postgraduate School. The spectrometer will be used both as an instructional aid for the optics and optoelectronics classes taught at the school, and as a medium resolving power, visible and near-ultraviolet instrument for future student thesis research. Development of the spectrometer was broken up into four areas: basic optical design, mechanical design and construction, optical alignment, and computer and electronic interface design and construction.

The optical design was done by using two commercially available computer programs: OSLO LT by Sinclair Optics, and OPTICA (an extension of Mathematica) by Wolfram Research, Inc. After designs of several configurations were analyzed, we chose a variant of the classic Ebert-Fastie design. Excluding the source and detector components, the optical portion of the spectrometer consists of a diffraction grating, two spherical mirrors, two flat mirrors, and two slits.

The mechanical portion of the project involved designing and building mounts for the diffraction grating and the slits, building spacers for all the optical components to set the optical axis of the spectrometer at the proper height, and designing and building a motor mount and gear box used to turn the diffraction grating in a precise manner.

Optical alignment and collimation of the spectrometer were done using a laser to set the positions and tilts of the mirrors and to define the optical axis, and a point source to set the entrance and exit slits at the proper foci of the two spherical mirrors.

The electronics used to control the spectrometer included a Compumotor controller for motor control, a Hewlett-Packard Data Acquisition/Switch Unit to sample the output of the detector, and a personal computer to interface the electronics and the spectrometer. The detector system was a conventional New Focus enhanced silicon photovoltaic detector, with wavelength coverage from approximately 350 to 1050 nanometers.

As a proof-of-concept demonstration, data was recorded for an iron hollow cathode light source. Spectral lines were graphed in Microsoft Excel and tentatively identified using published spectra of iron.

II. BACKGROUND

A. SPECTROMETER BASICS

The purpose of a spectrometer is to separate the light from a source into its component wavelengths and then to direct each component wavelength onto a detector where its characteristics can be measured. A simple block diagram describing this is shown in Figure 1 below.

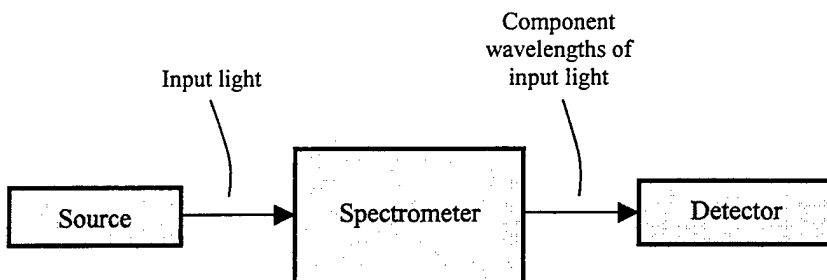


Figure 1. Simple block diagram of the spectrometer's function.

The optical layout for the spectrometer built during this thesis research is a variation of the classic Ebert-Fastie configuration [Ref. 1]. This configuration is shown in Figure 2. The primary advantage of the Ebert-Fastie design is that it self-compensates for spherical aberration, despite the fact that spherical mirrors are employed. The light from the source enters the spectrometer through the input aperture and strikes a spherical collimating mirror. The input aperture is located at the tangential focus [Ref. 2] of the collimating mirror. This mirror collimates the light and directs it to the diffraction grating. At the diffraction grating, the reflected light fans out into its component wavelengths, with each diffracted wavelength directed at a different angle. A spherical de-collimating mirror, identical to the collimating mirror, intercepts a narrow range of the

diffracted fan of light and focuses it onto the exit aperture and then onto the detector. Not shown in Figure 2 are auxiliary optics that collect light from the source and focus it onto the input aperture, or those optical components that focus light from the exit aperture onto the detector.

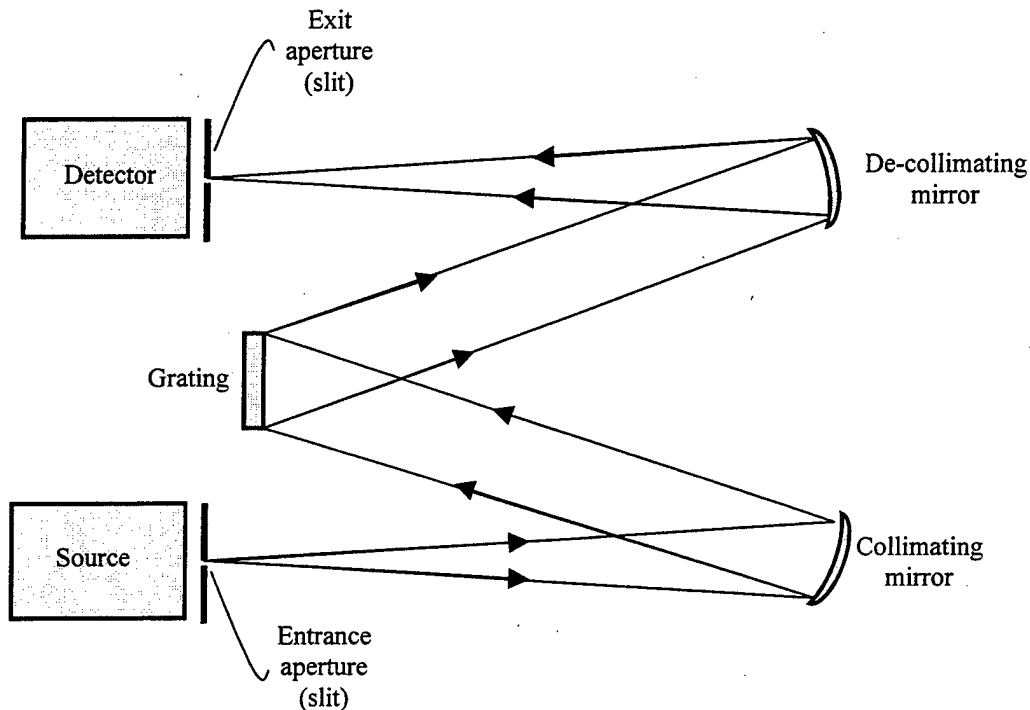


Figure 2. Ebert-Fastie spectrometer configuration.

B. DIFFRACTION GRATING

The heart of the Ebert-Fastie spectrometer is its diffraction grating. The diffraction grating is a repetitive array of diffracting elements, either apertures or obstacles, that has the effect of producing periodic alterations in the phase, amplitude, or both of an emergent wave [Ref.3]. The diffraction grating used in this spectrometer is a reflection grating. Its diffracting elements are a set of fine, parallel grooves, or rulings, in

a very smooth piece of aluminum-coated polymer on an optically flat glass surface. The diffracted light from a given ruling will travel to any point beyond the grating where it will interfere with light from the other rulings. If the geometry of the system is such that all the diffracted beams are in phase, then the system will transmit light of that wavelength to the detector.

The physics of the reflection phase grating can be seen in Figure 3. The gray vertical line represents the diffraction grating. The gray points represent the reflective diffractive elements, which are separated by a distance a . The incident light strikes the diffractive elements at an angle θ_i . The diffracted light leaves the diffractive elements at an angle θ_m . To find how the two incident light rays will interfere, the difference in

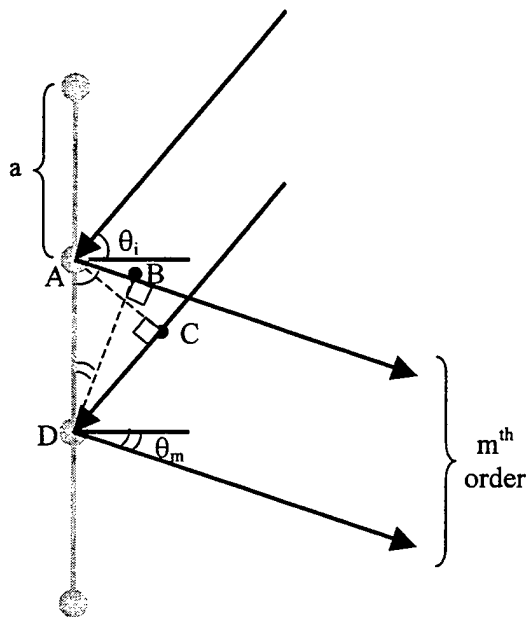


Figure 3. After Ref. [4]. A reflection grating.

distance traveled by each ray has to be determined. To find the path difference, determine the difference in the distance traveled from the wave front of the incident rays to the wave front of the diffracted wave. When the top ray is incident on the grating at point A, the lower incident ray is at point C. The line formed by the points A and C is perpendicular to the incident rays and represents the wave front of the incident wave when the top ray strikes the grating at point A. The line formed by B and D is perpendicular to the diffracted rays and represents the wave front of the diffracted wave when the lower incident wave strikes the grating at point D. The difference traveled by the two incident rays going from the incident wave front to the diffracted wave front is the path difference and is represented by AB - CD. Using the geometry of Figure 3, the path difference is

$$AB - CD = a(\sin\theta_m - \sin\theta_i). \quad (1)$$

The path difference will cause interference between the two rays due to the phase change caused by their travelling different distances. The rays will constructively interfere when their path difference is an integral value, m , of the incident wavelength, λ . Setting Equation 1 equal to the integral values of the wavelength gives the grating equation:

$$a(\sin\theta_m - \sin\theta_i) = m\lambda. \quad (2)$$

The integer m is called the order number (or simply order) of the diffracted beam. Notice that, when $m = 0$, $\theta_m = \theta_i$ and the grating acts like a conventional specular mirror,

reflecting all incident wavelengths at the same angle θ_m . For $m \neq 0$, however, only wavelengths whose $m\lambda$ satisfies Equation (2) will be reflected at angle θ_m .

Another property to note is that the smaller the grating spacing a is, the larger will be the diffraction angle θ_m . Therefore, for any given fixed geometry of the optical system, smaller grating spacing can produce fewer diffracted orders. For the diffraction grating used in this spectrometer, the grating spacing is 1200 lines/mm. Using the grating equation and the wavelengths for visible light, approximately 380nm to 760nm, it can be shown that only 3 or 4 orders will be diffracted. Figure 4 shows a typical picture of the visible orders for an incident angle $\theta_i = 20^\circ$, in which case 4 diffracted orders are produced.

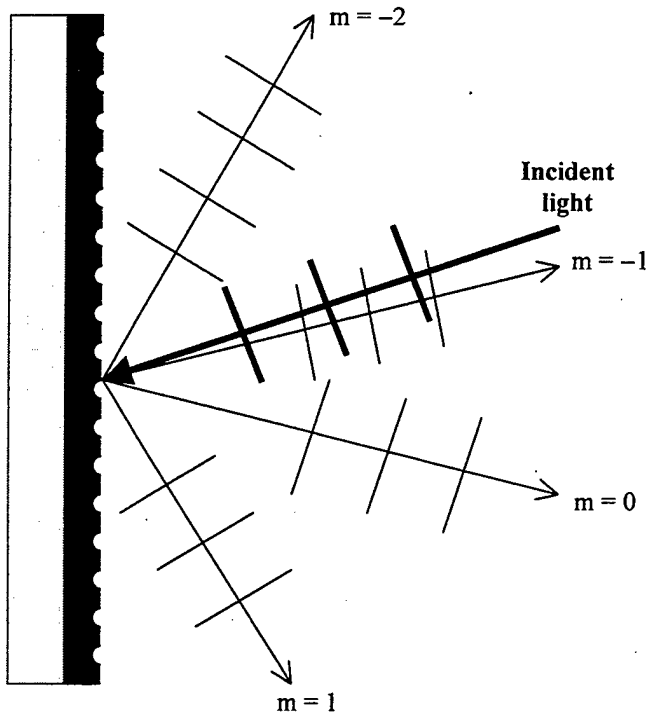


Figure 4. After Ref [4]. Diffraction grating orders for incident angle $\theta_i = 20^\circ$.

C. BLAZED DIFFRACTION GRATING

Detailed theoretical analysis [Ref. 5] shows that the order with the most light intensity occurs for the case of specular reflection from the grating's rulings. For the grating discussed previously, this occurs when $\theta_m = \theta_i$, or the $m = 0$ diffracted order. Because the actual spectrometer necessarily measures the intensity of the light in one of the nonzero orders of diffraction, (typically the $m = +1$ or -1), much of the light would be wasted. To compensate for this, the grating's rulings are typically shaped or angled to generate the effect of specular reflection in either the $m = +1$ or -1 orders. Gratings that incorporate this feature are said to be "blazed". Figure 5 shows a small section of the grating to illustrate the geometry describing how the blazed grating works.

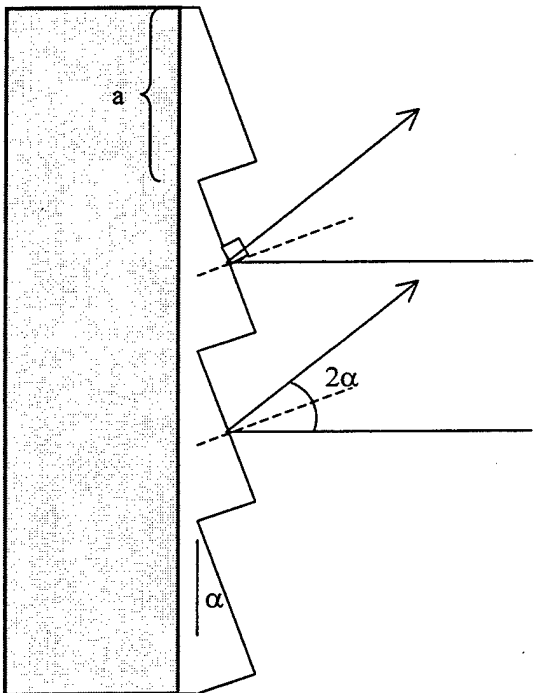


Figure 5. After Ref [6]. Blazed grating geometry.

The angular positions of the diffracted nonzero orders are still dependent on the grating equation, Equation (2). As before, the incident angle and the diffracted angles are measured from the surface normal of the diffraction grating, not the surfaces of the tilted rulings. Specular reflection off the rulings' surfaces, however, determines the maximum reflected light intensity. The angle α is introduced during the manufacturing process to produce this effect. For the case shown in Figure 5, the grating incident angle, θ_i , is zero, but the incident angle to the groove surface is α . The angle of specular reflection is 2α . Setting the diffraction angle, θ_m , equal to -2α and substituting it in to Equation (2), the grating equation becomes

$$a \sin(-2\alpha) = m\lambda. \quad (3)$$

The desired blaze angle, α , can then be determined for the desired diffracted order and wavelength from Equation (3). For the diffraction grating used in this spectrometer, the first order diffraction angle, θ_1 , is approximately 36° for wavelengths near the center of the visible spectrum. This corresponds to a blaze angle of $2\alpha \approx 36^\circ$.

THIS PAGE INTENTIONALLY LEFT BLANK

III. OPTICAL DESIGN

A. BASIC DESIGN CONSIDERATION

The primary objective in the design of any spectrometer is to achieve the greatest possible spectral resolving power and the largest spectral signal-to-noise ratio possible. These two goals are mutually exclusive.

The spectral resolving power of an instrument is defined as

$$R = \lambda / \Delta\lambda, \quad (4)$$

where λ is the average wavelength of two closely spaced spectral lines and $\Delta\lambda$ is their wavelength separation, assuming that they are barely resolved as two individual lines [Ref. 7]. Achievement of this goal requires careful control of the angular field-of-view of the instrument, using the smallest possible apertures consistent with diffraction-limited performance. That is, spectral resolving power is optimized by using small apertures in the instrument.

Maximizing the spectrometer's signal-to-noise characteristics, however, mandates that the greatest possible amount of light be collected by, and passed through, the instrument. This requires that the various apertures subtend the largest possible solid angles, which then necessitates use of the largest possible apertures. Clearly then, the design of a spectrometer is a trade-off between its ability to pass a lot of light (called its *etendue*, or optical throughput) and its resolving power.

Adding to the complexity of this design trade-off are ever present constraints imposed by the laws of optics. Finite optical elements generally produce both aberrations and diffraction effects. Consequently, there is no "right" design, only one that optimizes the trade-offs in a useful manner for a particular application. For purposes of this thesis project we chose to concentrate on an optical design that would employ off-the-shelf optical elements and fixed apertures, with the goal of maximizing the optical throughput by minimizing the instrument's optical aberrations. Further refinements to optimize overall performance were deferred to the future.

B. CONSTRAINTS

1. Diffraction Grating

The diffraction grating that was used was salvaged from a decades-old Littrow spectrometer. The specifications for the grating are listed in Table 1 below.

Length	$2 \frac{3}{32}$ "
Width	$2 \frac{3}{32}$ "
Lines/mm	1200
Blaze Angle	$36^\circ 52'$

Table 1. Grating specifications.

Because the grating is square, the ideal mirrors for the spectrometer would have been square ones of at least the dimensions of the grating. However, for reasons of cost, we chose to use circular mirrors instead of square ones. The length and width dimensions of the square grating give a diagonal of just over 2.5 inches. To take advantage of most of

the diffracted light from the grating, the spectrometer mirrors should have a diameter of approximately 2.5 inches. The blaze angle of the diffraction grating is $36^{\circ}52'$. Therefore to maximize the light energy diffracted to the detector, the incoming rays to the diffraction grating should make a $36^{\circ} 52'$ angle with the diffracted $m=1$ order rays going to the detector.

2. Available Commercial Optics

The use of commercially available optical elements was done to save time and money. We chose to limit the options for mirrors to inexpensive, readily available types from Edmund Scientific. There was a large selection of mirrors available with diameters ranging from 1 to 10 inches and focal lengths for the spherical mirrors ranging from 1 to 100 inches.

3. Space Constraints

The dimensions of the optical base plate on which the spectrometer was to be built is $88.5 \text{ cm} \times 119.5 \text{ cm}$. It is dotted with a grid of $\frac{1}{4} \text{ inch} \times 20$ threaded holes spaced evenly one inch apart along the length and width directions. Measuring from the center of the threaded holes, the usable dimensions of the optical base plate are $32 \text{ in} \times 44 \text{ in}$ (see Figure 6). It was estimated that approximately seven inches of the length dimension would be used for the source and detector components. This leaves a usable area of $32 \text{ in} \times 37 \text{ in}$ to build the spectrometer.

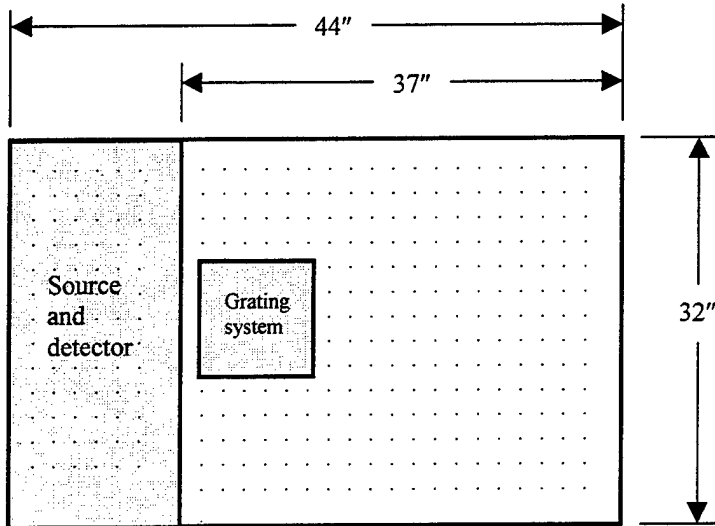


Figure 6. Optical base plate of spectrometer.

The diffraction grating is mounted on a rotating plate that allows it to scan the diffracted spectrum across the exit aperture. The rotator plate is turned by a drive motor and a reduction gear system. The rotator plate, motor, and gear reduction box will be discussed in more detail in the next chapter on mechanical design. The space requirements for the grating and its associated mechanical components was estimated to be approximately $10'' \times 10''$. Figure 6 shows the optical base plate with the source/detector area shaded gray along with the grating and its associated mechanical components (denoted as “grating system”) shaded gray. The white area is what is left for the remaining optical components of the spectrometer.

C. OPTICAL DESIGN

Using the constraints discussed above, optical components were selected to design a basic Ebert-Fastie spectrometer like the one shown in Figure 2. Three inch diameter spherical mirrors with focal length $f = 30$ in were chosen for the collimating

mirrors. This design fills a rectangle approximately 20 in \times 30 in on the optical base plate, as shown in Figure 7. The design goal was to minimize the system's optical aberrations at the exit slit. Placing spherical mirrors at angles to the incoming light

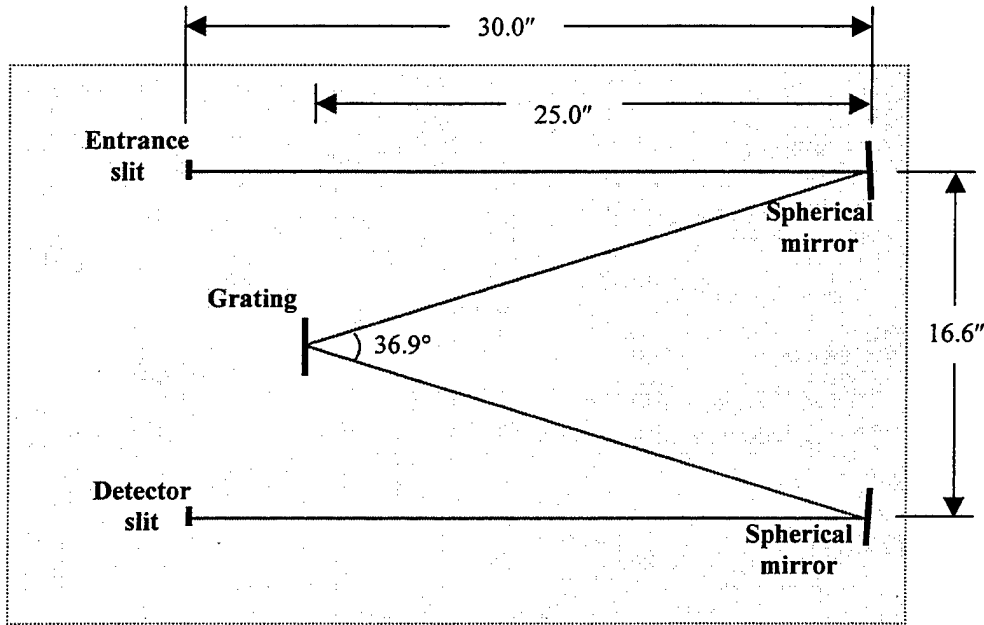


Figure 7. First design of Ebert-Fastie spectrometer, without folding mirrors.

introduces astigmatism and spherical aberrations. In general, minimizing the tilt angle of the spherical mirrors can reduce the effects of astigmatism, and proper matching and focusing of the collimating mirrors will minimize spherical aberration. Because of the size of the grating system and the blaze angle of the grating, reducing the off-axis tilt angle of the spherical mirrors in this original spectrometer design is not practical. Another way to reduce the off-axis tilt angle is to add two flat mirrors to fold the

reflected light from the spherical mirrors. A second design was made to incorporate such folding, using two 3-inch diameter flat mirrors as shown in Figure 8.

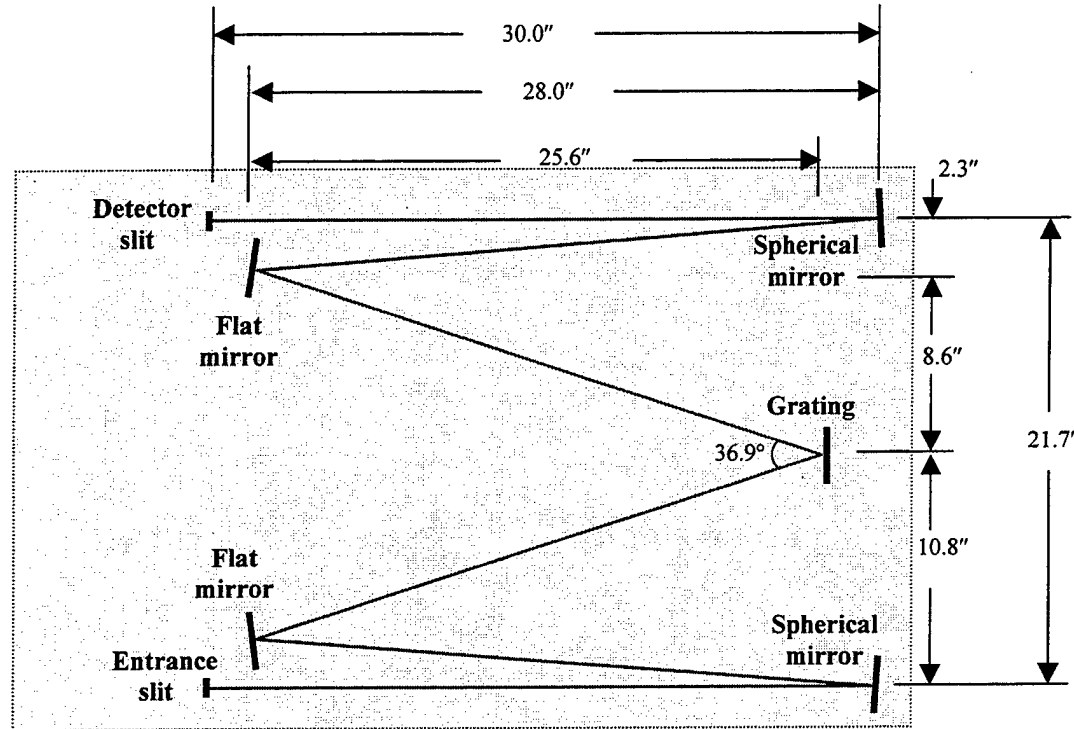
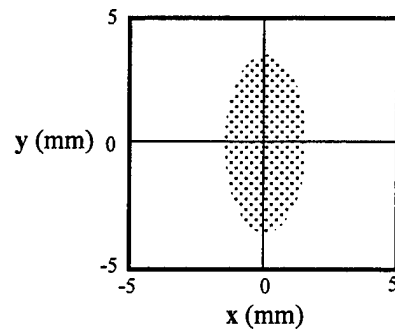
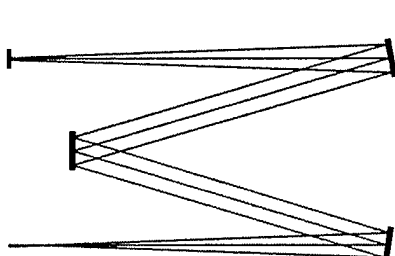


Figure 8. Second design of Ebert-Fastie spectrometer, with folding mirrors.

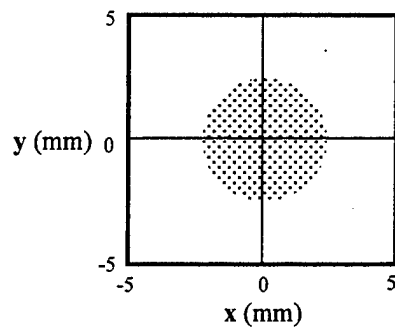
D. OPTICAL DESIGN SOFTWARE

Two different versions of commercially available design software were used to analyze the proposed optical layout of the spectrometer. Both were capable of being run on a desktop personal computer. The first was OSLO LT Optical Design Software. OSLO stands for Optics Software for Layout and Optimization, and is distributed by Sinclair Optics. We used a free version downloaded from the Internet. It was limited to

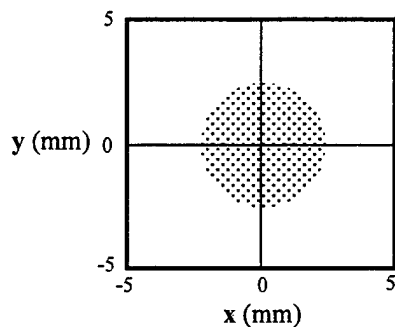
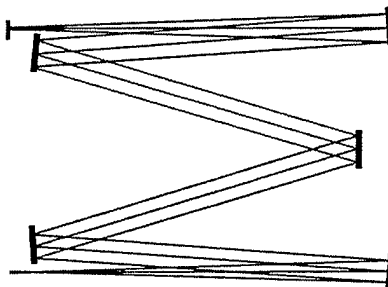
12 surfaces, which was enough to analyze the folded version of the Ebert-Fastie spectrometer. The spectrometer designs were entered into a spreadsheet, and ray trace and spot diagram analyses were done. Figure 9 summarizes the raytrace and spot diagram analyses for three designs.



a) Ebert-Fastie first design (unfolded).



b) Ebert-Fastie first design revised to reduce aberrations.

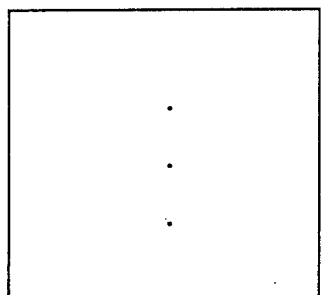


c) Ebert-Fastie folded design to reduce aberrations.

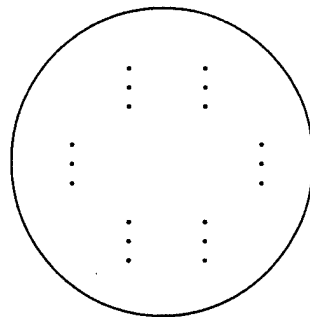
Figure 9. OSLO LT ray trace and spot diagram summary.

The hypothetical entrance aperture was a 5 mm diameter circle. A circle instead of a slit was used in order to make it easier to see the aberrations. The spot diagrams correspond to ray intersections with the exit slit plane. In Figure 9a, it's apparent that the spot diagram is severely distorted due to aberrations. Reducing the off-axis tilt angle does reduce the aberrations as seen in Figure 9b. However, this design is not optimal for the blaze angle of the grating, nor does it leave enough room for the mechanical components of the grating system. Figure 9c displays the final folded design, which was arrived at via several iterations. This design reduces the aberrations to acceptable levels and still allows sufficient room for the grating system mechanics. Hence, this was the design that was adopted.

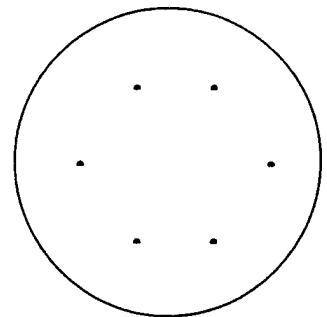
The second optical design software package that we used was OPTICA by Wolfram Research, Inc. It is an application that runs under Mathematica. This was used as an independent check on the accuracy of the OSLO-generated design of the folded Ebert-Fastie spectrometer. A ray trace and spot diagram analysis was done by allowing three rays to propagate from the entrance slit to the exit slit. Figure 10 shows the spot diagram as the rays encounter each optical element of the spectrometer. This spot diagram analysis determined that residual aberrations would produce an output point spread function whose width is $50\mu\text{m}$ at the spectrometer's exit slit. This implies that the exit slit width should be on the order of $50\mu\text{m}$. For simplicity, we chose a symmetrical entrance slit also with a width of $50\mu\text{m}$. The OPTICA analysis also confirmed that the folded Ebert-Fastie design was a feasible design.



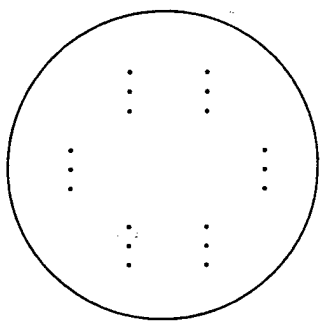
a) Entrance slit



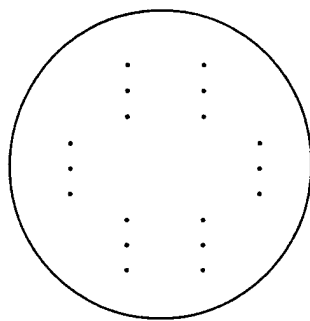
b) Collimating mirror



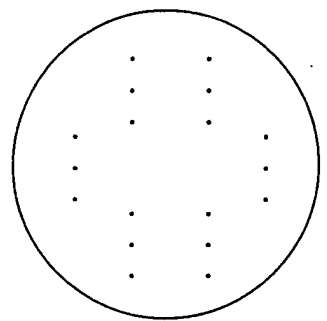
c) First folding mirror



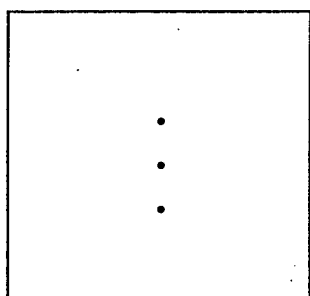
d) Grating



e) Second folding mirror



f) De-collimating Mirror



g) Exit slit

Figure 10. OPTICA spot diagram analysis.

THIS PAGE INTENTIONALLY LEFT BLANK

IV. MECHANICAL DESIGN

A. OPTICAL MOUNTS

Commercially available optical mounts were purchased to accommodate the two flat and two spherical mirrors. Figure 11 is a rear view picture of one of the mounts. The mirror slides in from the front and is held in by a small radial setscrew within the frame. The two control knobs allow for tilt adjustment about the horizontal and vertical axes. There are two counterbored holes through the bottom of the mount to allow attachment to a base.

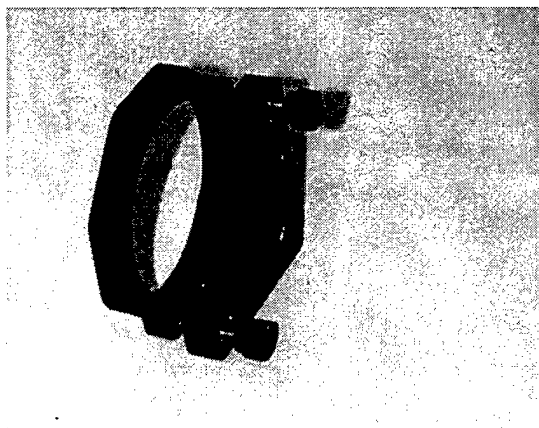


Figure 11. Mirror mount.

The diffraction grating was too big to fit in an off-the-shelf 3" mount, so a custom mount had to be designed and built to house the grating. Its parts included a sturdy frame and a compression washer backing to hold the grating against the frame. The design drawings for the diffraction grating frame are in Appendix A. Figure 12 shows a picture

of the grating in its mount sitting atop some substrate components that are discussed in the next section.

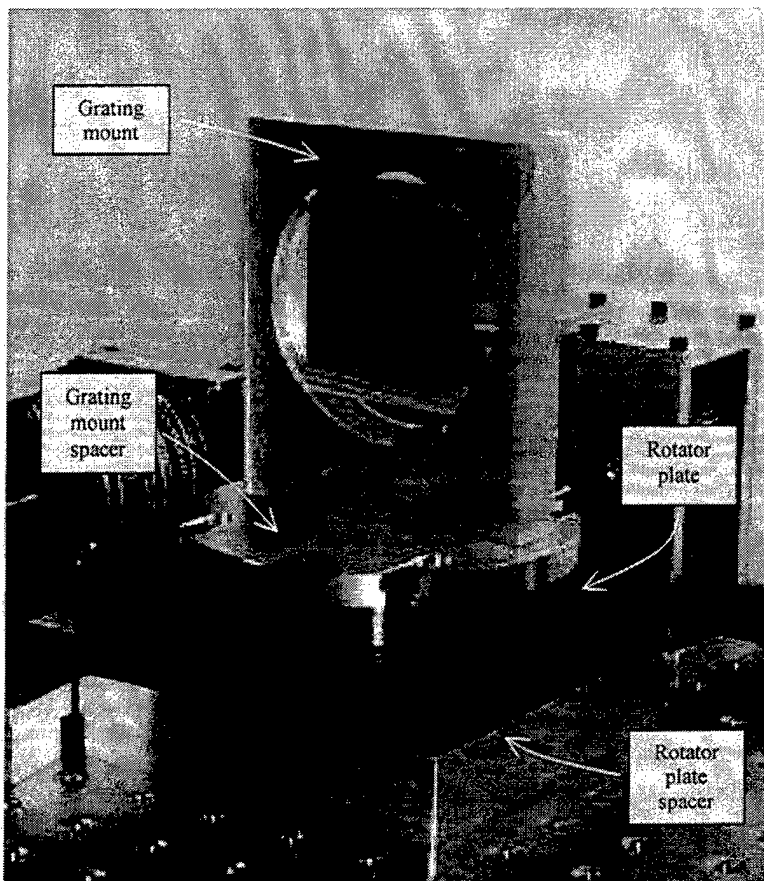


Figure 12. Diffraction grating mount, rotator plate and their spacers.

B. SPACERS

The optical elements of the spectrometer all have to be located with their optical axes above the base plate. To allow for ample mechanical clearance of all components, an optical axis height of 5" was chosen. This required that spacers be made for the various mounts. The spacers for the mirror mounts were made out of aluminum plate and consisted of two parts fastened together. The drawings for the spacers are in Appendix

A. Figure 13 shows a mirror in its mount attached to its spacer assembly and dogged to the optical base plate.

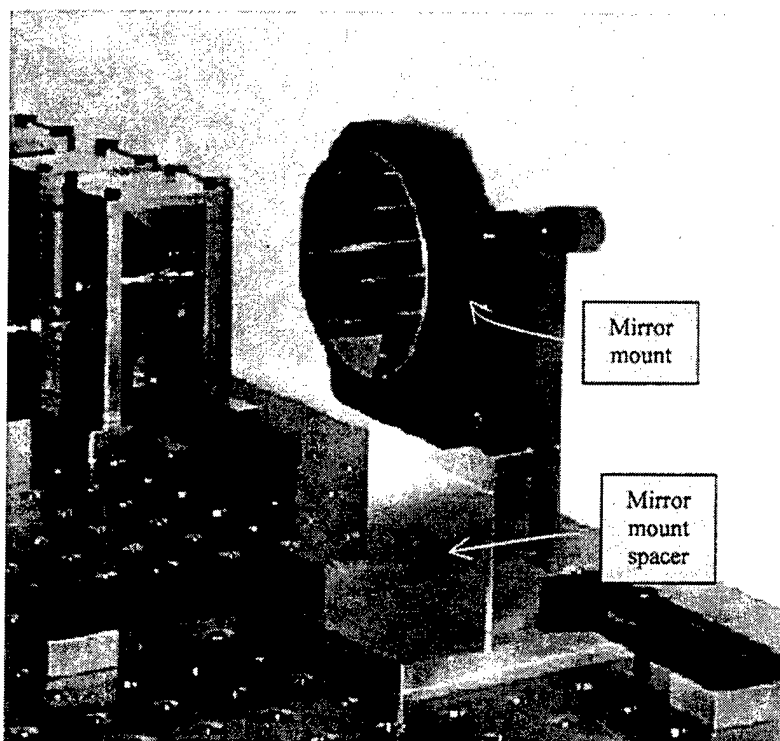


Figure 13. Mirror in mount atop spacer.

The spacer for the grating mount was a little more complex in design because it had to interface the opto-mechanical rotator plate with the grating mount and permit the centering of the grating face coincident with the axis of rotation. The grating mount spacer was made out of $3/8"$ aluminum plate and has slotted holes to attach it to the rotator plate. This allows precise adjustment of the grating's surface above the axis of rotation of the rotator plate. The grating mount spacer is visible in Figure 12, just below

the grating mount atop the rotator plate. The drawing for the grating mount spacer is included in Appendix A.

C. ROTATOR PLATE

The commercially available rotator plate is shown in Figure 14. It consists of a 4.75" \times 4.75" base with a 4.75" diameter turntable on top. The bigger knob visible in the foreground is the manual turning actuator. 180 turns of the actuator shaft generates one revolution of the turntable via a precision worm gear drive. The smaller knob is a lock for the turntable. In the actual spectrometer, both knobs are removed, and the actuator shaft is turned with a motor drive system.



Figure 14. Rotator plate.

A 1" aluminum plate spacer was placed under the rotator plate to raise it so that a gear could be attached to its actuator shaft to allow it to be mechanically driven by a motor. Its corresponding drawing is in Appendix A. Figure 12 shows the rotator plate atop the rotator plate spacer.

D. ENTRANCE AND EXIT SLITS

In keeping with the optical aperture designs discussed earlier, slit-shaped entrance and exit apertures were made by placing two single edged razor blades 50 μ m apart. The slit width calibration was done using a visible diode laser while observing the single slit diffraction pattern produced by the slit [Ref. 8]. Aluminum mounts were made to hold the razor blades and to place the center of each slit on the optical axis. The drawing for the slit mounts is in Appendix A. Figure 15 shows one of the razor blade slits on its mount.

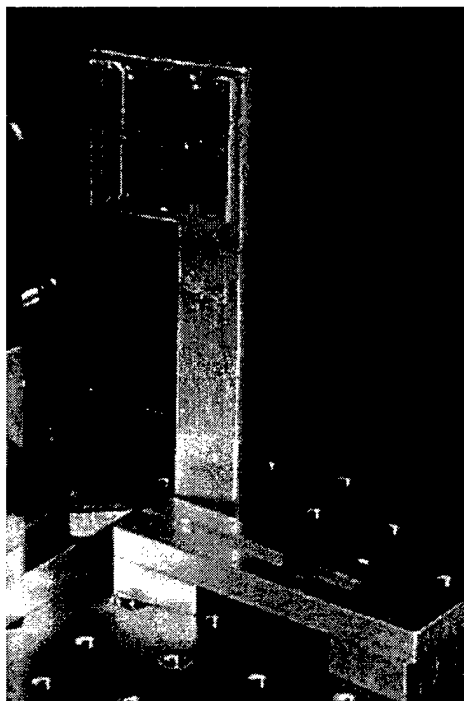


Figure 15. Razor blade slit on mount.

E. MOTOR AND GEARBOX

A gearbox was needed between the stepping motor and the rotator plate's actuator shaft. First, it serves as a mechanical interface. Second, it is needed to decrease the step size to ensure that each motor step does not translate the spectrum by more than the width of the instrumental line shape at the exit slit. Were such large steps to occur, it would be possible for the spectrometer to step completely over, and thereby to miss recording, some of the spectral lines. A calculation was done to determine the amount of gear reduction needed. It is shown below. It assumes that each motor step turns the motor shaft 1.8° . This was the specific step increment of the original motor to be used.

- Rotator plate turns 2° for every complete revolution of the actuator shaft.
- Stepping motor turns 360° for 200 motor steps.
- Rotator plate rotation/motor step (without reduction gearing) = $0.01^\circ/\text{step}$ or $1.75 \times 10^{-4} \text{ rad}/\text{step}$.
- The optical moment arm from the grating, to the folding mirror, to the collimating mirror, and then to the exit slit is approximately two meters. Therefore, the change in the position of the center of a monochromatic spectral line at the exit slit with each unreduced motor step would be $1.75 \times 10^{-4} \text{ rad}/\text{step} \times 2 \text{ meters} = 350 \mu\text{m}/\text{step}$.
- The designed instrumental line width is approximately $50 \mu\text{m}$. So to ensure adequate sampling of the spectrum, the displacement of a monochromatic line at the exit should not exceed $25 \mu\text{m}/\text{step}$. Therefore the gearing ratio for the drive system should be roughly $350 \mu\text{m}/25 \mu\text{m}$ or 14:1.

The motor finally chosen for the spectrometer is a Compumotor AX-57 model stepping motor. This motor turns 360° for every 12,800 steps. Even without reduction

gearing, this motor would generate a line displacement of $5.5 \mu\text{m}/\text{step}$ at the exit slit. However, because of mechanical run-out and jitter, we chose to incorporate a gear reduction system, with a drive ratio of 6.55:1. A toothed belt drive and pinion system was designed, rather than a direct gear-to-gear configuration, in order to minimize mechanical backlash in the system. Figure 16 illustrates the reduction gear setup schematically and Figure 17 is a photograph of the actual system.

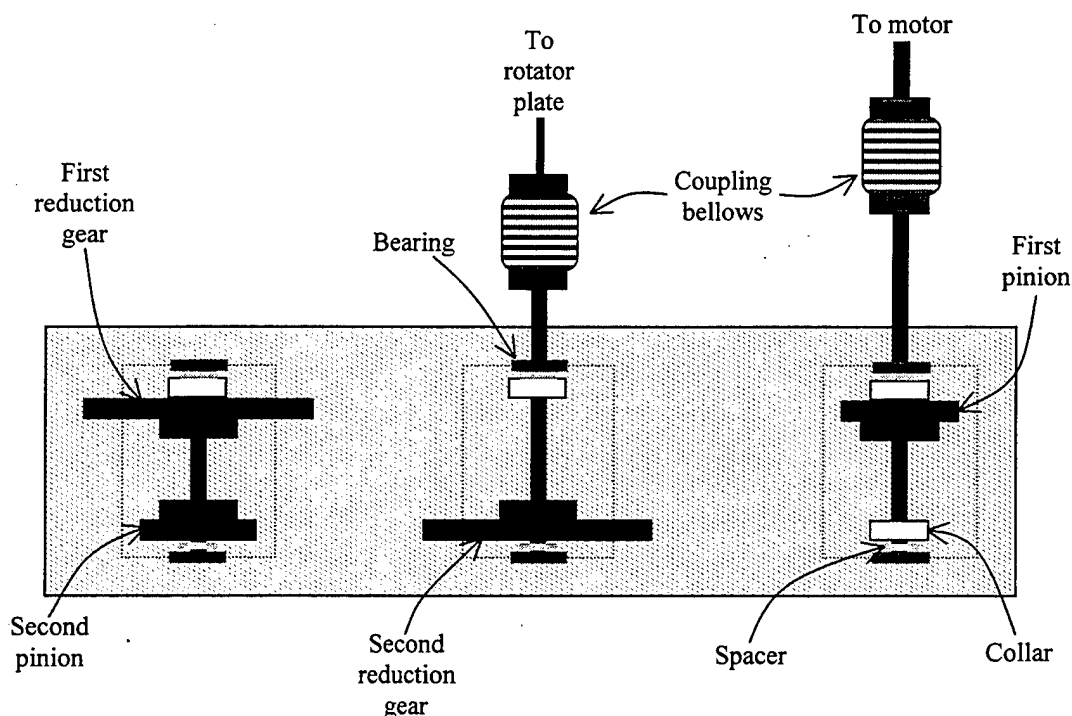


Figure 16. Reduction gear schematic.

In Figure 16, the large gray box represents the base plate of the gearbox. The three dotted boxes inside the gear box represent the top view outline of the gear box frames that support each of the three shafts via the bearings shown. The motor shaft is

coupled to the first pinion by a coupling bellows. The first pinion is coupled to the reduction gear by a toothed fiberglass belt. The second pinion turns with the first reduction gear and is coupled to the second reduction gear by another toothed fiberglass belt. The pinion gears are both 25 tooth gears and the reduction gears are both 64 tooth gears, which gives the overall gear reduction ratio of 6.55:1. This non-obvious ratio was established merely by the availability of commercial gears and belts. The second reduction gear turns a shaft that is coupled to the rotator plate actuator via a coupling bellows. All shafts are $1/4$ " diameter shafts with the exception of the rotator plate actuator shaft, whose diameter is $1/8$ ".

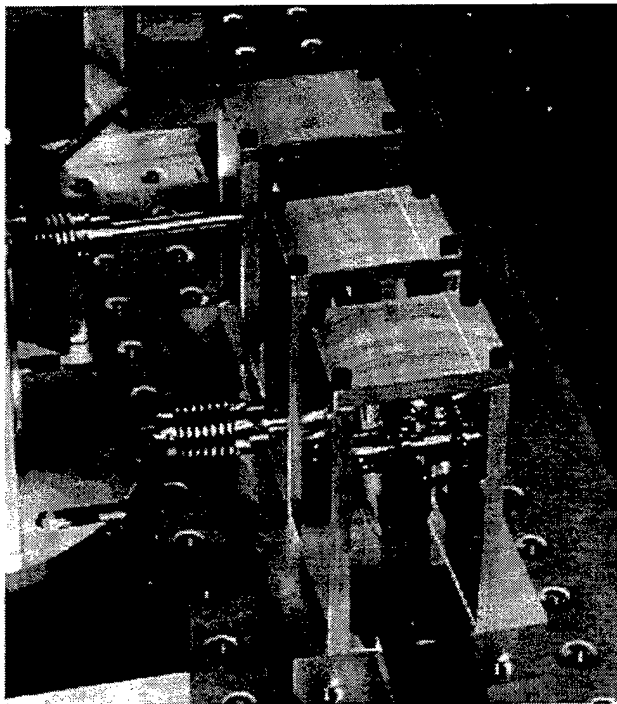


Figure 17. Gearbox and reduction gear system.

F. ASSEMBLY

As the key mechanical component in the entire instrument, the rotator plate and its spacer were screwed directly to the optical base plate, and the positions of all other components were established relative to it. All other components were fastened to the optical base plate with mechanical dogs and blocks. Figure 18 shows a top view of the complete assembly with all mechanical components in place. Not shown are several baffles that prevent outside light from entering the spectrometer and also inhibit optical cross talk between the different optical components.

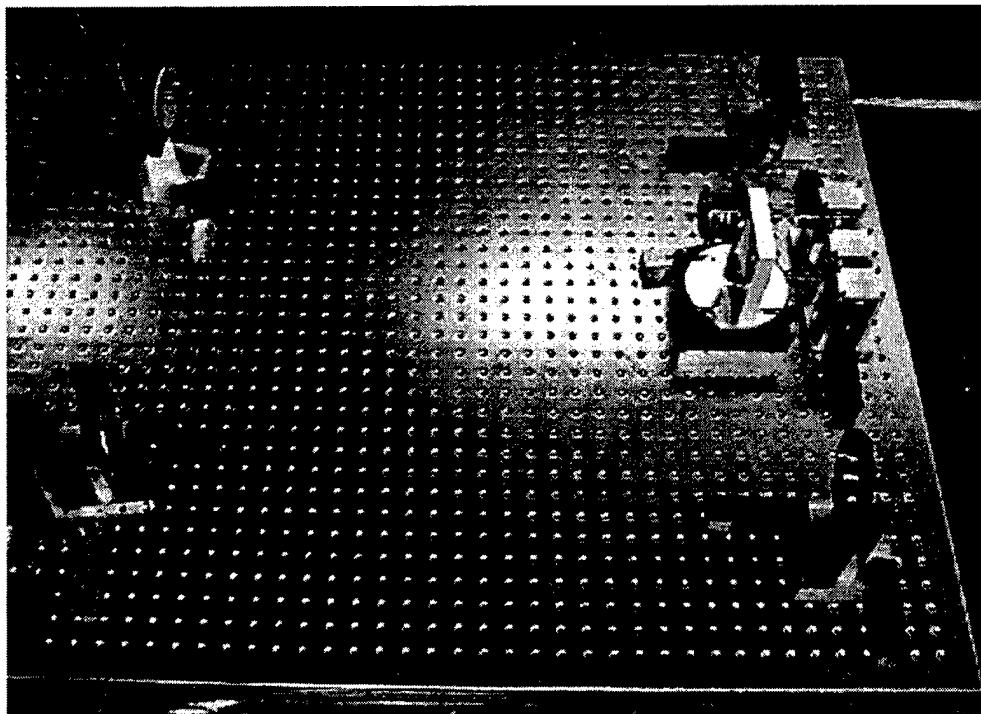


Figure 18. Top view of spectrometer.

THIS PAGE INTENTIONALLY LEFT BLANK

V. SPECTROMETER ALIGNMENT

In any high precision optical instrument, very careful attention must be paid to the optical alignment of its components if good performance is to be achieved. This means that the utmost care must be taken in establishing and stabilizing the mechanical positions and tilts of the various optical elements in the system.

As discussed earlier, all of the components in the spectrometer have their positions and orientations established relative to the diffraction grating, which, in turn must be aligned with its surface coincident with the rotation axis of the mechanical drive. So, the first optical alignment task was to position the grating and its drive system.

A. ALIGNMENT OF THE DIFFRACTION GRATING

There are two critical parameters that must be established in aligning the grating. First, the rotation axis of the grating drive must be brought into coincidence with the grating's ruled surface. Second, the rulings themselves must be made parallel with the rotation axis. Both of these constraints insure that the optical beam will remain focused and stable at the exit slit.

Therefore, the first part of the spectrometer alignment required placing the grating face exactly on the axis of rotation of the rotator plate. Precise measurements of the radii of the rotator plate and the grating spacer followed by subtracting the residual offsets in their radii, accomplished this to within 0.001" tolerance. The results are shown in Figure 19. The grating frame was designed to be fastened to the grating spacer with the grating's face on the centerline of the grating spacer. By knowing the difference in the radii of the rotation plate and grating spacer, the grating spacer could be adjusted such

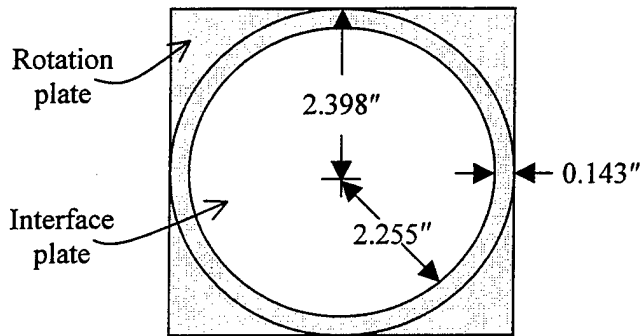
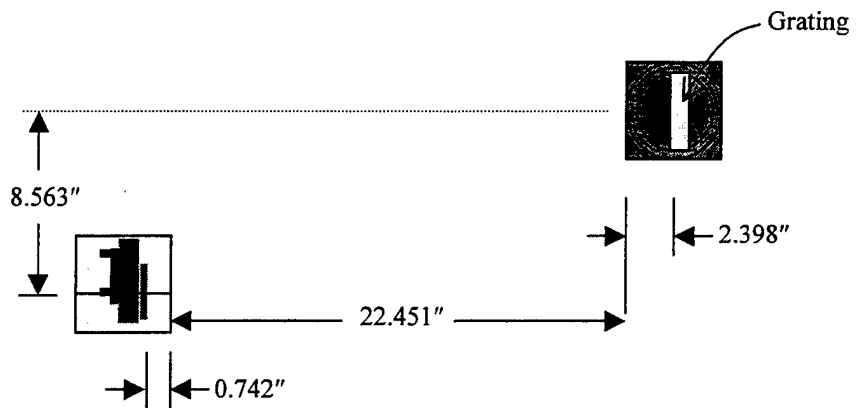


Figure 19. Top view of dimensions of rotator plate and grating spacer.

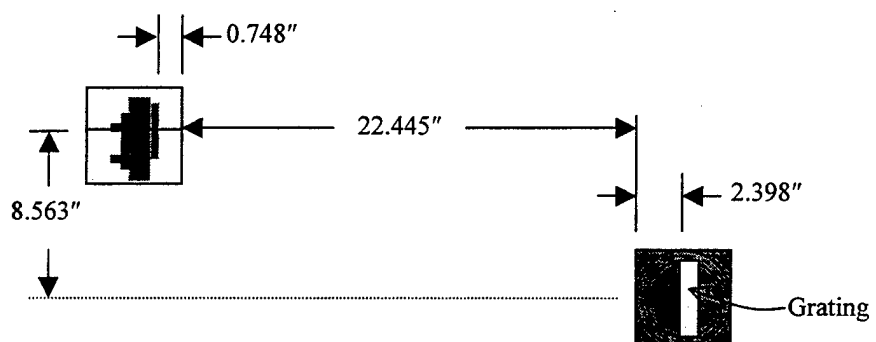
that its edge was 0.143" from the edge of the rotation plate, thus placing the face of the grating at the axis of rotation to within the tolerance of the mechanical gauges used. The rotator plate and its spacer were then directly screwed to the optical base plate.

B. ALIGNMENT OF MIRRORS

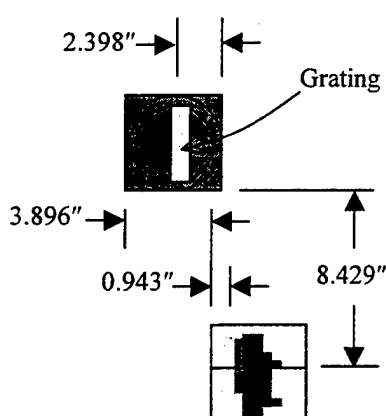
The mirror positions were established by offsets from the grating rotation axis, using the design dimensions shown in Figure 8 and precise machinist's gauges. This is harder to do than it would seem. All the mirrors are elevated on mounts and spacers. This makes it difficult to place them in their exact positions because of the mechanical offsets between their optical surfaces and mount bases. To make positioning easier, the dimensions of each of the spacer's bases were measured with respect to the optical axis of each of the mirrors. Then the mirrors could be placed into position by locating their spacers on the base plate. Figure 20 summarizes the final mirror placement dimensions with respect to the diffraction grating's rotation axis.



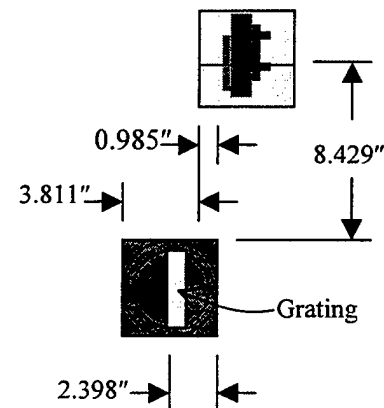
a) Source side flat mirror position.



b) Detector side flat mirror position.



c) Source side spherical mirror.



d) Detector side spherical mirror.

Figure 20. Mirror positions with respect to grating position.

Once the mirrors were located in their proper positions, their tilt orientations had to be established. This was done with the aid of a laser, which was set up on the optical base plate as shown in Figure 21.

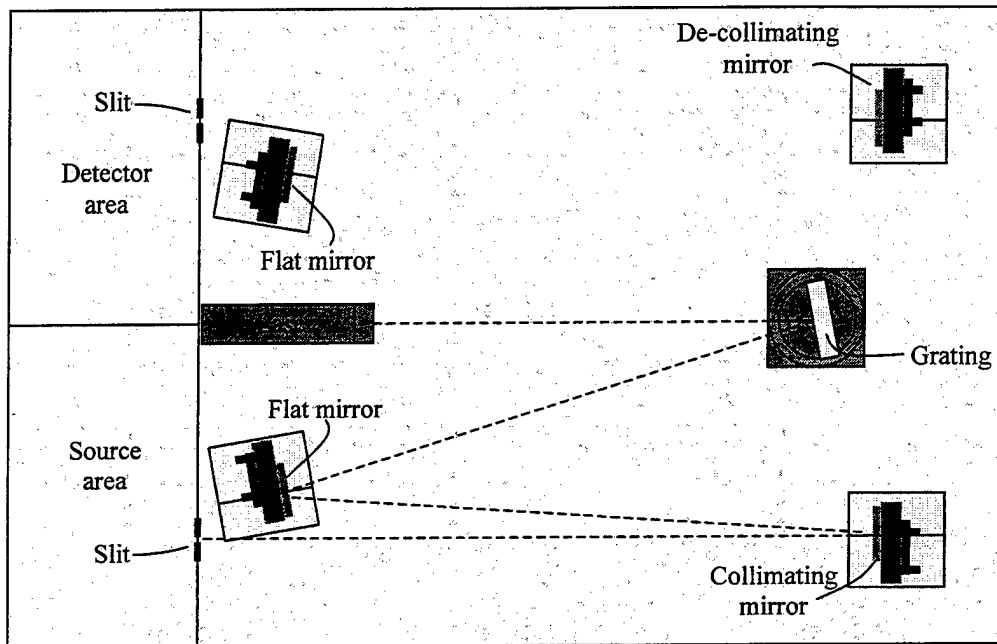


Figure 21. Optical tilt alignment using laser.

The laser was put on jacks to adjust the height of the beam to 5", the height of the spectrometer's optical axis. A machinist's height gauge was used to ensure the laser beam height was as close as possible to the nominal value of 5". First, the grating was spun within its mount and the heights of the various diffracted beams were checked to be 5" to insure that the grating rulings were perpendicular to the base plate, thus insuring that the diffracted beams were parallel to the surface of the base plate. Then the laser was aimed at the center of the diffraction grating and the grating was rotated so that the laser beam would strike the center of the flat mirror as shown in Figure 21. Again the height

gauge was used to verify that the height of the beam was 5" near the diffraction grating and near the flat mirror. The flat mirror was then tilted to aim the beam at the center of the collimating mirror. The tilt was adjusted in both altitude and azimuth so that the laser beam was 5" in height near the flat mirror and near the collimating mirror. The collimating mirror was then tilted to send the beam toward the source slit, with subsequent tweaking of the mirror's tilts to keep the laser beam at its nominal 5" height and parallel to the base plate. The same process was then done with the diffraction grating rotated to align the two mirrors on the detector side of the spectrometer.

C. POSITIONING OF SLITS

The focal lengths of the spherical collimating mirrors had to be verified to ensure the slits were at the optimum focal positions. This was done by collimating a zirconium arc point light source then observing the zeroth-order diffracted image at each slit. The setup for the source side is shown in Figure 22. A lens collimates the light from the point source. After reflection from the grating and flat mirror, the light then propagates to the collimating mirror as shown in Figure 22. Ideally the collimating mirror focuses an image of the point source onto the slit. The slit is positioned to coincide with the smallest and sharpest image that can be found. Experimentally, the focal length for each of the spherical mirrors was approximately a half inch larger than the advertised 30" value, so the slit positions were adjusted accordingly from their designed locations.

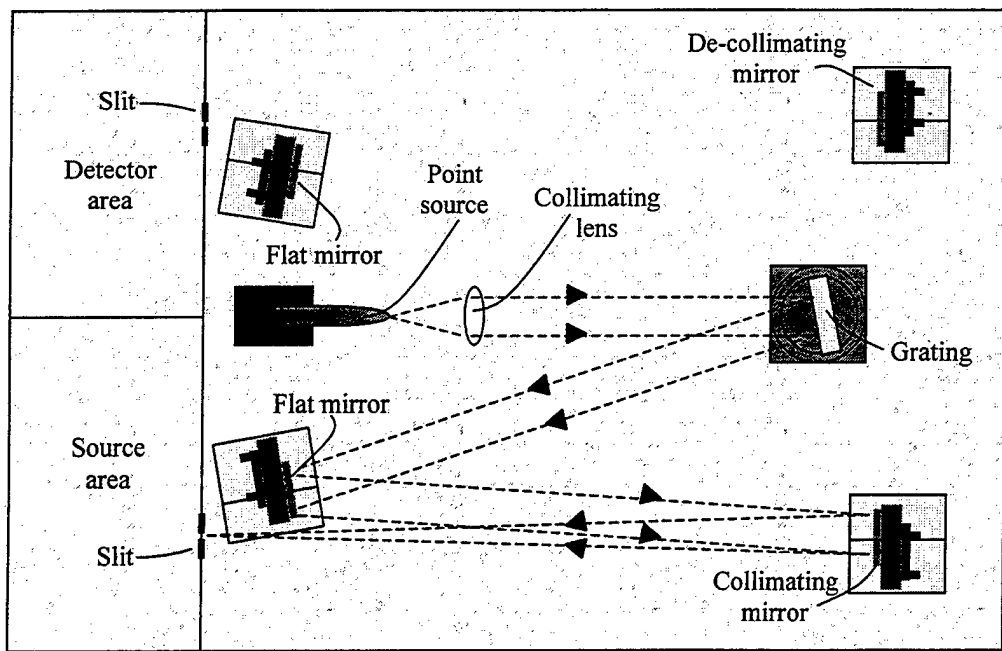


Figure 22. Setup to position slits.

VI. SPECTROMETER CONTROL AND DATA ACQUISITION SYSTEMS

In order to take economical advantage of existing mechanical, opto-mechanical, electronic and computer hardware, the spectrometer's control and data acquisition systems were configured as simply as possible. The resulting configuration is not optimal for an instrument of this type, but it is sufficient to demonstrate that the spectrometer works as designed.

At the heart of the system is a personal computer, which is responsible both for controlling the stepping motor that drives the grating and for acquiring and displaying the spectral data. There are also several additional components, including a spectroscopic light source, opto-mechanical chopper, opto-electronic detector/amplification module, lock-in amplifier, and computer-controlled data logger. The roles of these various components are discussed below.

A. MOTOR AND MOTOR CONTROLLER

The motor that turns the diffraction grating is a Compumotor A/AX57-51 two phase permanent magnet hybrid stepping motor. It, in turn, is driven by a Compumotor Microstep Drive AX-Series controller. It is a bipolar microstepping drive designed for 12,800 steps per motor shaft revolution. The controller is interfaced to the PC via an RS-232 serial interface operating at 9,600 baud [Ref. 9]. A Visual Basic [Ref. 10] program was written to control the motor. The graphical user interface for the program is shown in Figure 23. The control program provides only the simplest functions needed for

spectrometer operation: motor enable/disable, motor speed, and motor direction. The code for the program is enclosed as Appendix B.

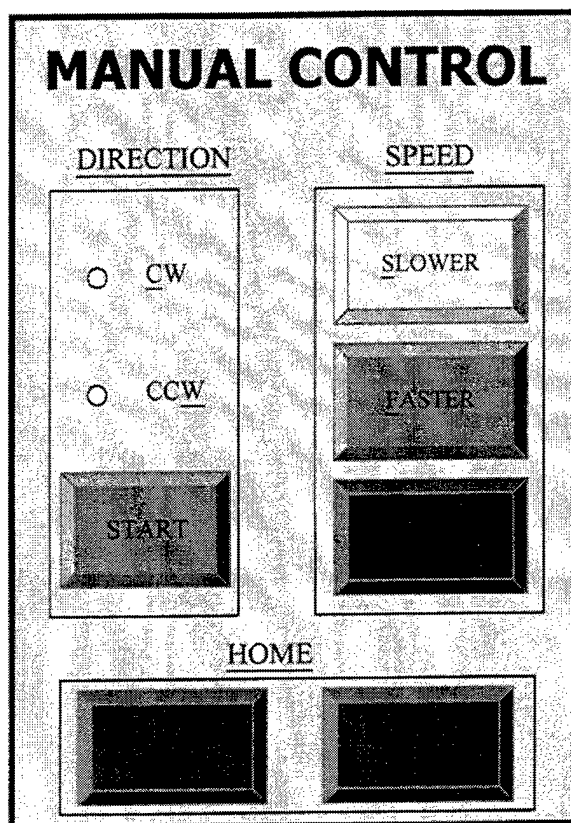


Figure 23. User interface for motor control program.

B. LIGHT SOURCE

The spectroscopic source lamp used for testing of the spectrometer is a Starna iron hollow cathode lamp. A DC power supply, adjustable current regulated lamp supply, and a switch are required for lamp operation. The lamp is shown in Figure 24. The lens and flat mirror constitute the spectrometer's foreoptics, collecting light from the source and focusing it onto the entrance slit, about the optical axis. After the light is reflected by the

flat mirror, it passes through a chopper before striking the entrance slit. The chopper is part of the detector system and will be discussed next.

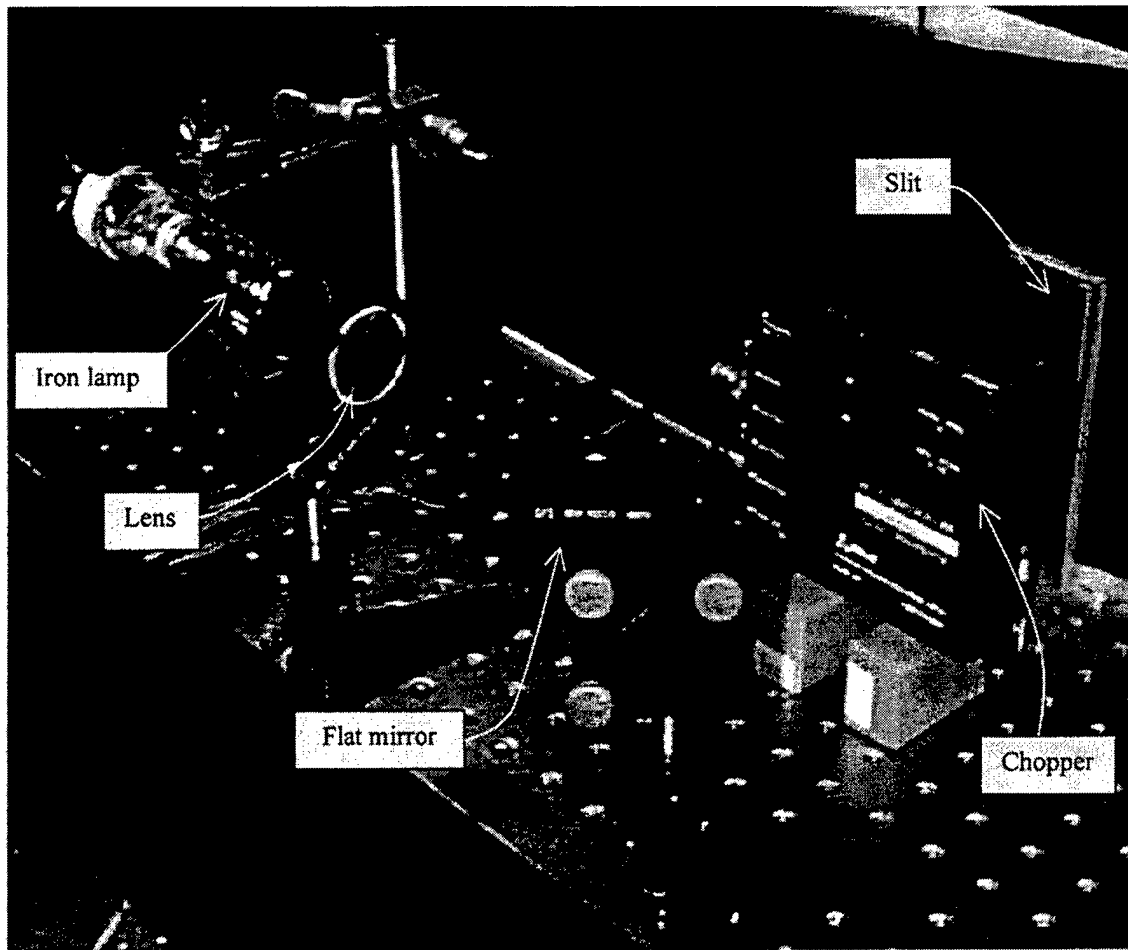


Figure 24. Spectrometer source, foreoptics and chopper.

C. DETECTION SYSTEM

1. Detector

The detector used is a silicon photodiode plus transimpedance amplifier module, made by New Focus, Model 2151. It's advertised spectral wavelength range is 300nm to 1050nm. The detector unit is battery powered and incorporates an extremely high gain

amplifier that makes it ideal for low light level detection [Ref. 11]. A lens was placed in front of the detector to focus the light from the exit slit onto the 1mm diameter detector area. Figure 25 shows the detector and lens setup.

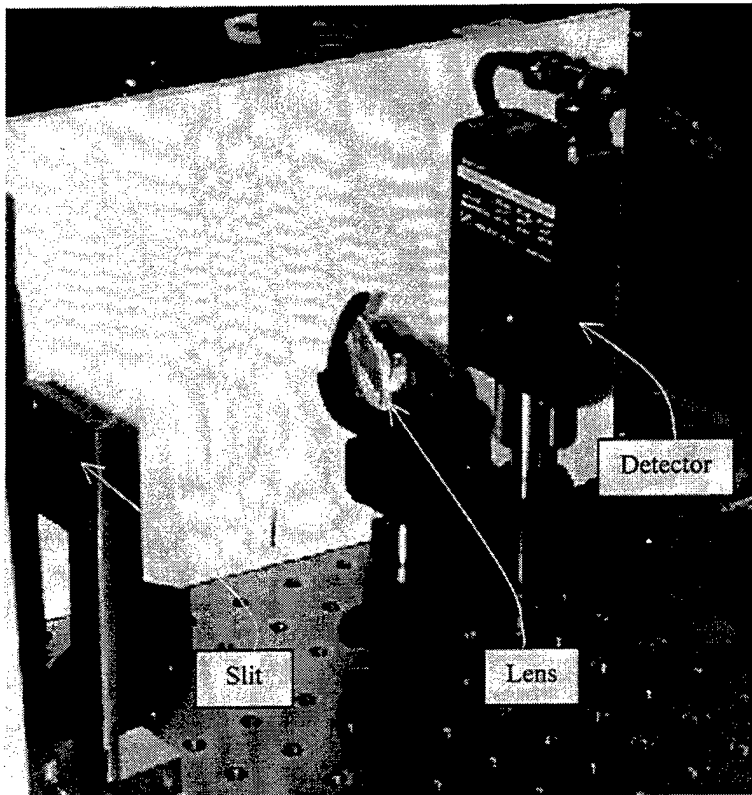


Figure 25. Spectrometer detector.

2. Lock-in Detection

Lock-in detection was used to improve the sensitivity of the detection process. Figure 26 shows a block diagram of a simple lock-in detection system. In Figure 26, the “Experiment” block represents the spectrometer. The “Weak signal + noise” symbol denotes the detector output. The detector is subject to 1/f noise. 1/f noise is worse for

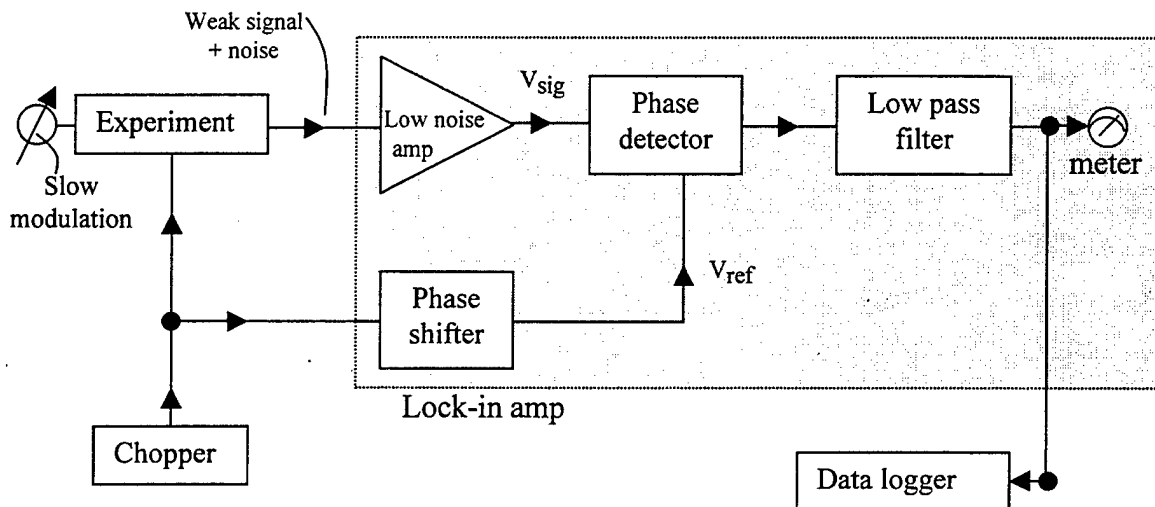


Figure 26. [From Ref. 6] Lock-in detection.

DC signals, which implies that the signal being detected needs to be modulated minimize this effect. This is done with a chopper, consisting of spinning disk with periodic holes at a constant radius where the light passes through. The spinning disk impresses a square wave amplitude modulation (AM) onto the incoming optical beam. The frequency of this modulation is set to a low-noise region of the detector's electrical passband. Figure 27 shows a hypothetical detected signal at the modulated frequency. For prototype testing of the spectrometer, a 500Hz modulation frequency was used.

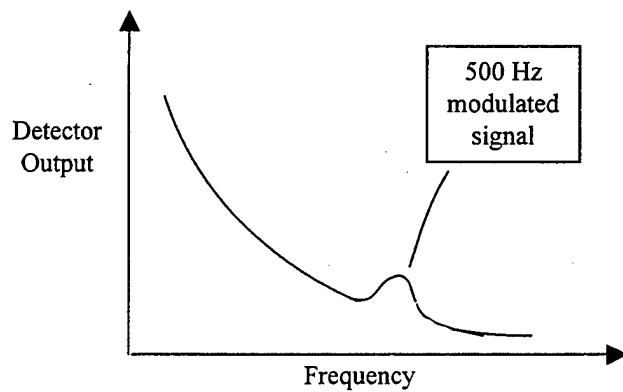


Figure 27. Detector output versus frequency.

The detector output and the chopper frequency are both input into the lock-in amplifier. There the detector output is amplified by a low noise amplifier and then passed to a phase detector that compares the phase of the detector's signal to that of the chopper signal. The relative phase shift between the chopper signal and the detector's signal is nulled, then the two are multiplied together by the lock-in to produce AM demodulation of the chopped optical signal. To first order, the demodulated signal is a DC signal proportional to the detector's signal level at the chopper frequency. The net effect is the production of a DC signal proportional to the optical signal level, plus heterodyne sidebands at any noise frequencies present. The signal is then sent to a low-pass filter, which rejects the noise sidebands and passes the desired signal. The pass band $\Delta\omega$ of the filter is user-selectable as the reciprocal of the low pass filter time constant τ . Using the method of lock-in detection essentially generates a relatively noise-free signal from a signal that was originally many, many dB below the ambient RMS noise level. The output of the low pass filter goes to displays on the lock-in amplifier's panel and to the data logger, as shown in Figure 26.

3. Data Logger

The data logger has the responsibility of acquiring the analog output of the lock-in amplifier, converting it to digital form, and buffering it to the host PC. The one used in this project is the HP 34970A Data Acquisition/Switch Unit. The HP 34970A utilizes plug-in modules for various applications. For this application, the HP 34901A 20 Channel Multiplexer module is used to record the voltage output from the lock-in

amplifier. The HP 34970A comes with the HP Benchlink Data Logger software which is a Windows-based application designed to make it easy to use the HP 34970A with a personal computer. The software allows for set up of test, acquiring and archiving measurement data, real time display and analysis of data, and copying measurement data and graphics to a file or clipboard for use in other applications [Ref. 13]. Figure 28 illustrates the detector system block diagram and its interface with the data logger and computer.

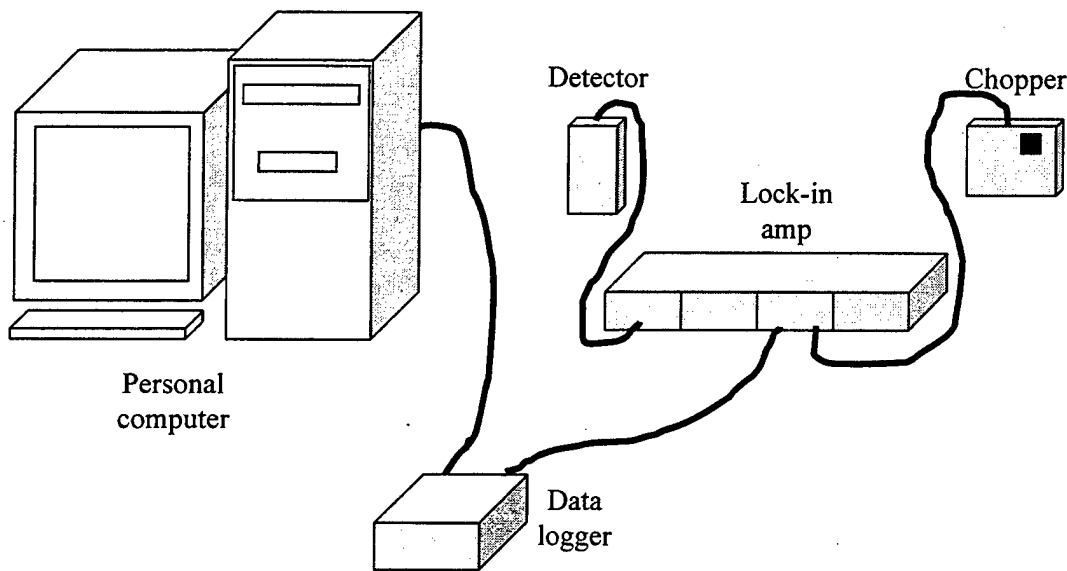


Figure 28. Detection system block diagram.

THIS PAGE INTENTIONALLY LEFT BLANK

VII. VERIFICATION OF OPERATION AND DATA ACQUISITION

After all of the spectrometer's subsystems were assembled, tested, and aligned, an overall proof-of-concept demonstration was conducted. The results of that demonstration are summarized in this chapter.

A. DETERMINING GRATING ANGLE

In Chapter 2, a derivation of the grating equation was done. In order to calibrate the wavelengths measured by the spectrometer, that derivation must be carried one step further to include the geometry of the spectrometer grating drive to determine diffracted wavelength as a function of grating rotation angle. The grating rotation angle, φ , is defined as the angle between the grating normal and the axis of symmetry of the spectrometer as shown in Figure 29. The incident beam and the diffracted beam each make an angle ϕ with respect to the symmetry axis, as shown. ϕ is constant with respect to the symmetry axis because it depends on the position of the collimating and flat mirrors, which are fixed in position on the optical base plate. Returning to the grating equation (see Equation 2), when the grating rotates by angle φ , the incident angle and diffraction angle are $\theta_i = \phi + \varphi$ and $\theta_m = \phi - \varphi$ respectively. Substituting these into Equation (2), the grating equation, gives:

$$m\lambda = a(\sin(\phi - \varphi) - \sin(\phi + \varphi)). \quad (4)$$

Using trigonometric identities for the sine terms, equation (4) reduces to:

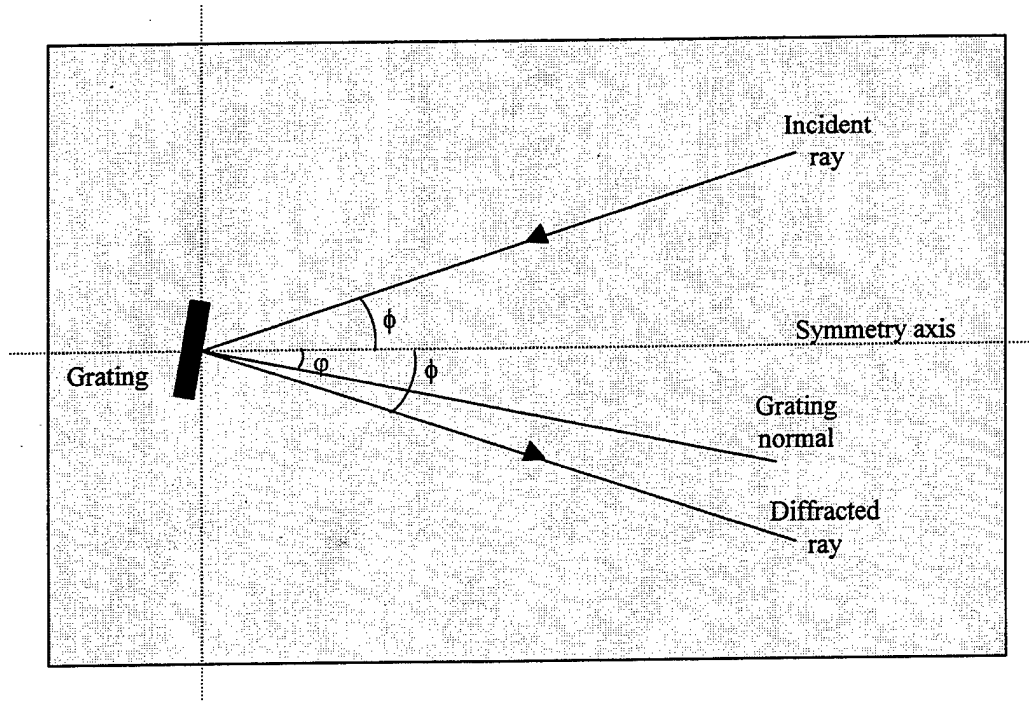


Figure 29. Grating rotation angle geometry.

$$m\lambda = -(2a)\cos\phi \sin\phi, \quad m = 0, \pm 1, \pm 2, \dots \quad (5)$$

Solving for the grating rotation angle gives us Equation (6), which will allow us to calculate the rotation angle of the grating for a given wavelength of light and order of diffraction, or conversely, the detected wavelength as a function of ϕ :

$$\phi = \pm \arcsin(m\lambda/(2a \cos\phi)). \quad (6)$$

For the iron spectral emission line used, the expected wavelengths were determined from the published literature [Ref. 16]. The detector response covers a wavelength range of roughly 300nm to 1050nm. Using Equation (6), the grating rotation

wavelength range of roughly 300nm to 1050nm. Using Equation (6), the grating rotation angle range corresponding to the detector's spectral coverage was determined to be 10° to 35° , assuming first order ($m=1$) diffraction. The starting grating angle placement was facilitated by fastening a protractor to the top of the spectrometer and putting a reference pointer at the 0° grating rotation angle position as shown in Figure 30, below.

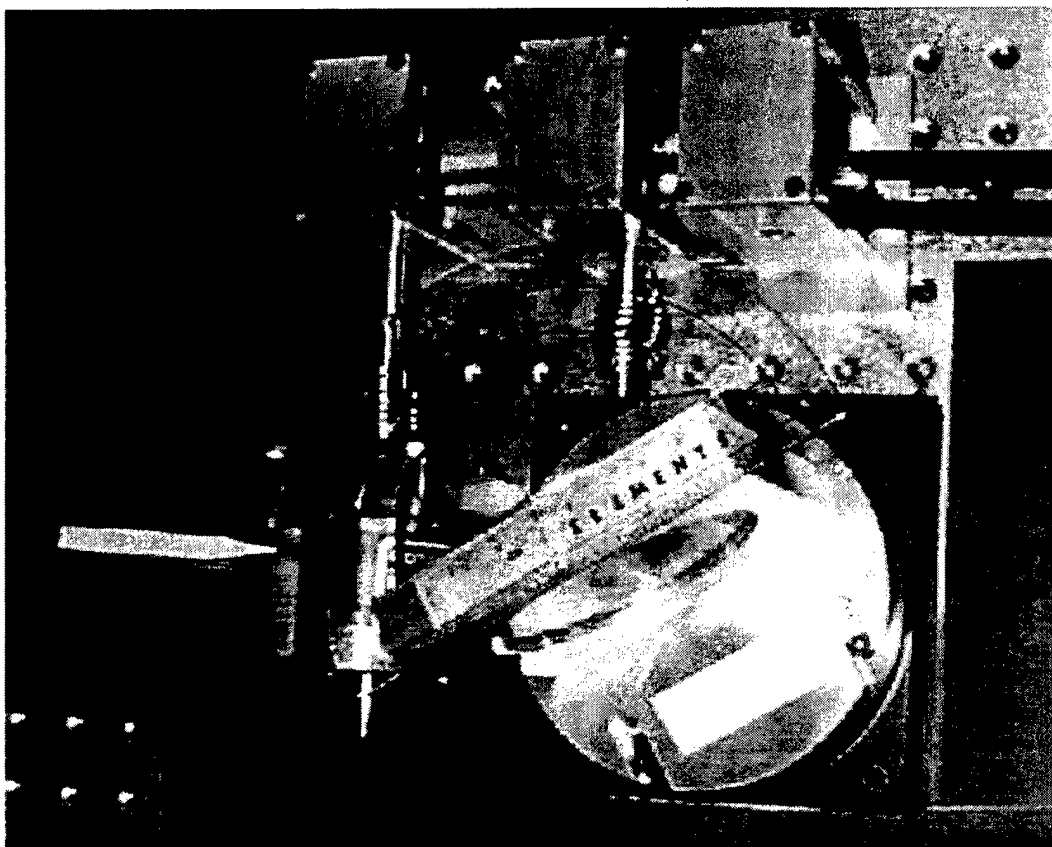


Figure 30. Top view of diffraction grating with protractor and reference pointer.

B. SPECTROMETER OPERATION

This section will overview the basic scenario for operating the spectrometer to obtain data. Power has to be supplied to all of the following equipment: light source,

grating motor and controller, detector system components, including the detector, chopper, and lock-in amplifier, HP 34970A Data Acquisition/Switch Unit, and personal computer. On the personal computer, the Visual Basic program for grating motor control has to be run and the HP data logger software for recording data has to be run. Using the Visual Basic program for manual motor control, the grating can be placed at the desired initial rotation angle, as discussed in the previous section. With the grating at the correct starting rotation angle, the data logger software can be invoked to start scanning the detector output and the motor can be turned on. Data will be displayed numerically both on the data logger workspace and graphically on the screen of the computer. When the grating has reached the final rotation angle, data acquisition is stopped by user interaction with the data logger program, and the motor is stopped using the motor control Visual Basic program. The data can then be looked at graphically using the data logger program and/or it can be saved to a ASCII disk file. The file can be loaded subsequently into a spreadsheet or other data processing program.

C. REPRESENTATIVE SPECTROMETER DATA

As a demonstration, data was measured for the Fe hollow cathode lamp across a grating rotation angle range of 10 to 35 degrees. This corresponded to a wavelength range of approximately 300nm to 900nm for order $m=1$. The data acquisition sample rate was 10 samples per second and the diffraction grating was turned at a rate of 0.916° per minute. This data run took approximately 30 minutes to complete. Figure 31 shows an Excel chart [Ref. 15] of the data as detector output vs. calculated wavelength. To

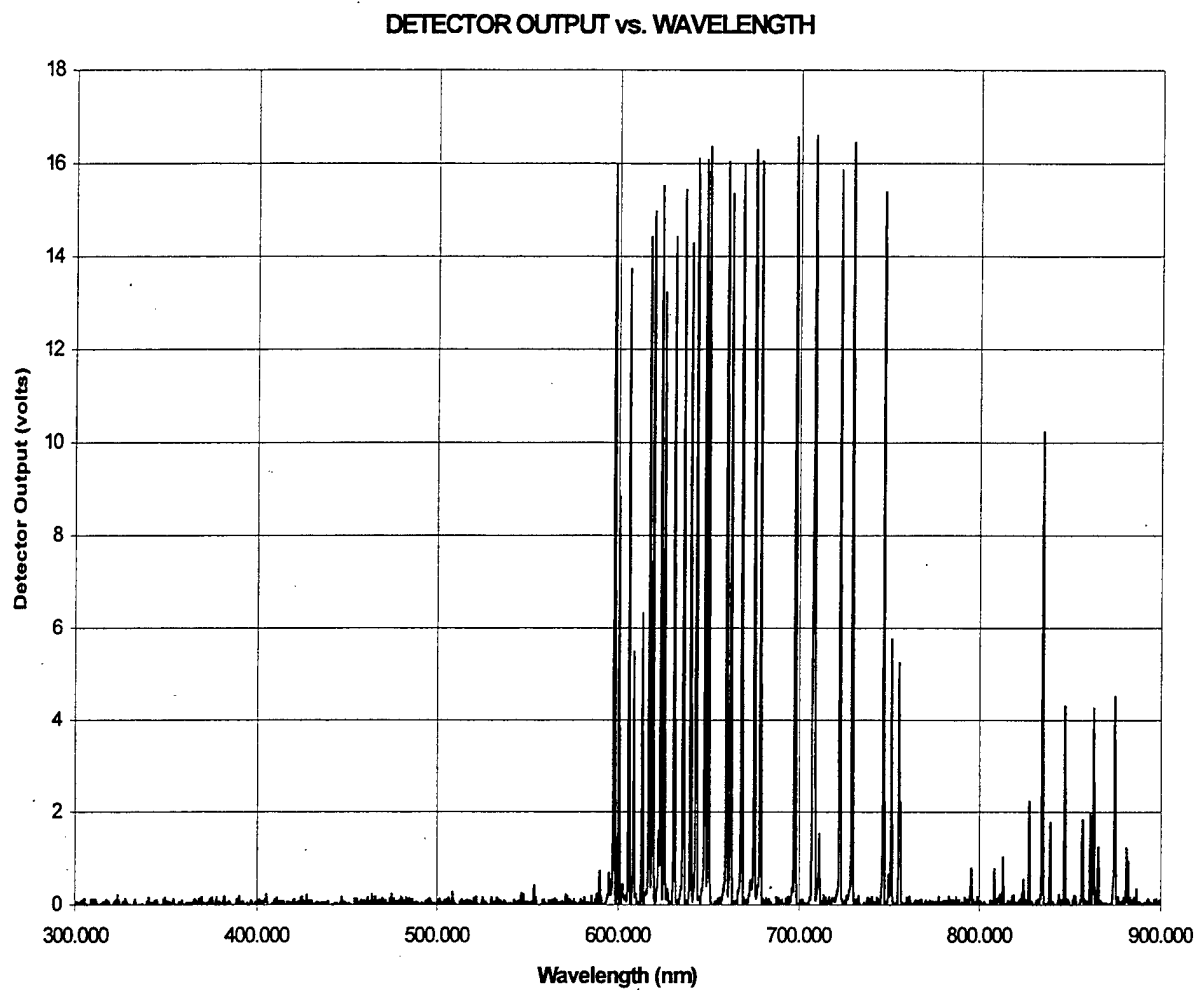


Figure 31. Detector output verses calculated wavelength

tentatively identify the iron lines, the data was plotted over a smaller wavelength band for comparison with the tabulated iron line data. The wavelengths labeled on the graph are only for order $m=1$. It is possible to detect higher order lines at the same grating rotation angle, in which case the actual wavelength would be shorter by a divisor equal to the absolute value of the order number $|m|$. For instance, a hypothetical $m=1$ line at 700 nm would coincide with an $m=2$ line at 350 nm, an $m=3$ line of 233.33 nm ...and so forth.

In Appendix C, a table summarizes the recorded data and its tentative iron line identification using the published literature [Ref. 16]. Unless otherwise noted, the identified lines are all due to Fe I (un-ionized iron). There are few lines that did not correlate with the published Fe spectrum. Some of them can probably be attributed to other elements close to Fe in the periodic table because of the chemical difficulty in purifying iron.

VIII. CONCLUSIONS

An Ebert-Fastie spectrometer was designed, built and tested using the constraints of commercially available optics, a pre-existing reflection diffraction grating, and a standard optical base plate. The design was independently verified and optimized using two optical design software packages, OSLO LT by Sinclair Optics and OPTICA by Wolfram Research. The optical mount for the diffraction grating, the entrance and exit slits, motor mount, gear box, and matching spacers were designed and built in-house at the Naval Postgraduate School Physics Department machine shop. A Visual Basic program was written to control the spectrometer's drive motor under computer control. HP Data Logger software was used in conjunction with the HP 34970A Data Acquisition Unit and lock-in detection to produce a data acquisition system. As a demonstration, the system recorded the spectrum of a Fe hollow cathode source. The measured data was compared to a published Fe spectrum, verifying that the spectrometer functions properly.

The spectrometer developed during this thesis research is a first-generation prototype unit. As such, we have identified several areas for potential improvement and refinement. Further suggested work includes:

- Design and build more substantial light baffles to replace the temporary foam plastic baffles currently used. Design and build a light-tight cover for the entire spectrometer.
- Optimize the resolving power of the spectrometer by checking the point spread function with a laser and measuring the line shape for different entrance and exit slit widths, altering the slit characteristics accordingly.

- Investigate and correct observed electrical ground loops associated with the chopper, motor, and/or detector systems.
- Design and build more sophisticated foreoptics to optimize the optical throughput from various spectroscopic light sources to the spectrometer's entrance slit.

Completion of each of these tasks promises to yield substantial improvements in the spectrometer's sensitivity and resolving power.

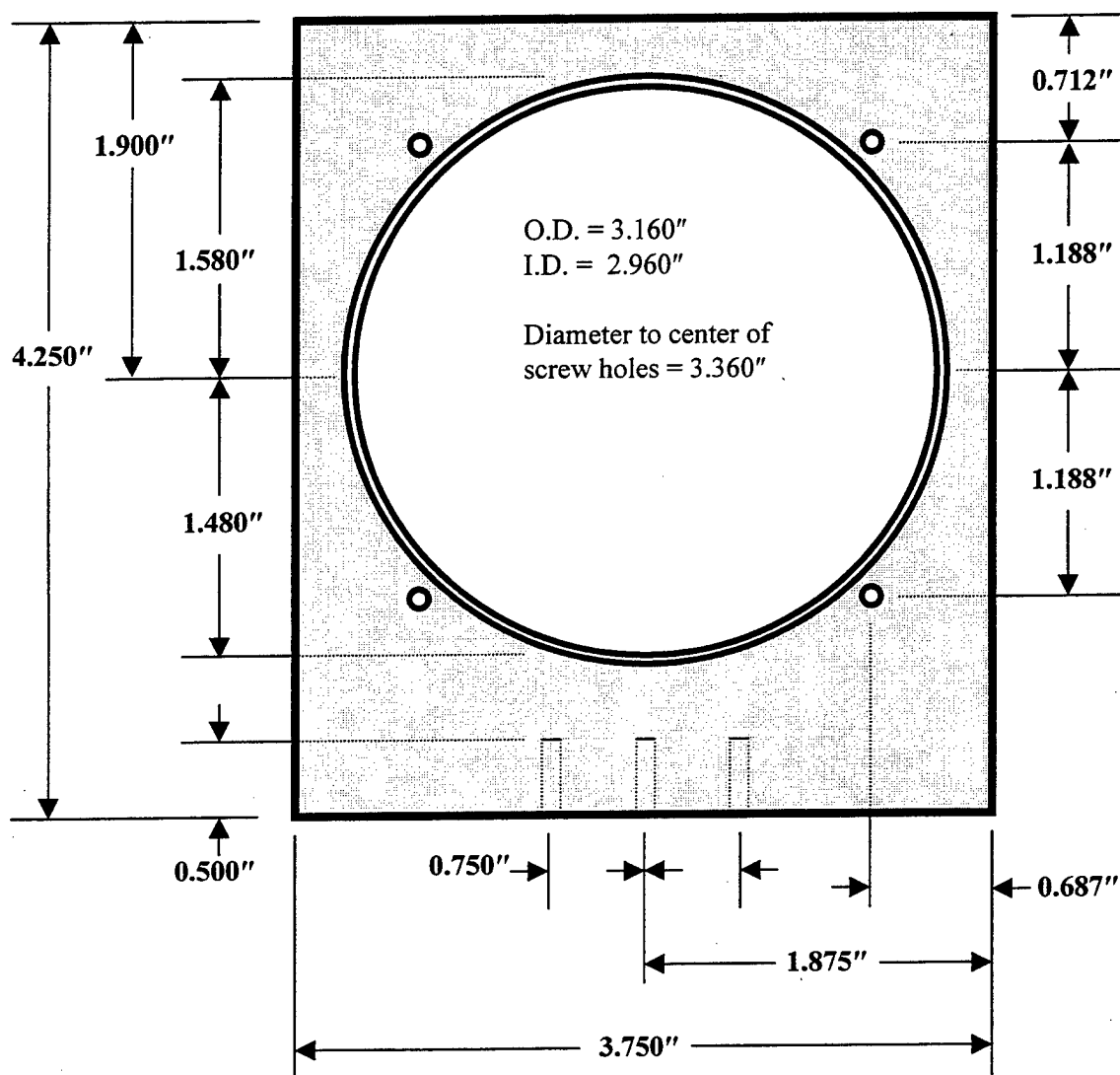
APPENDIX A. DRAWINGS

Design drawings for the mechanical systems built for the spectrometer

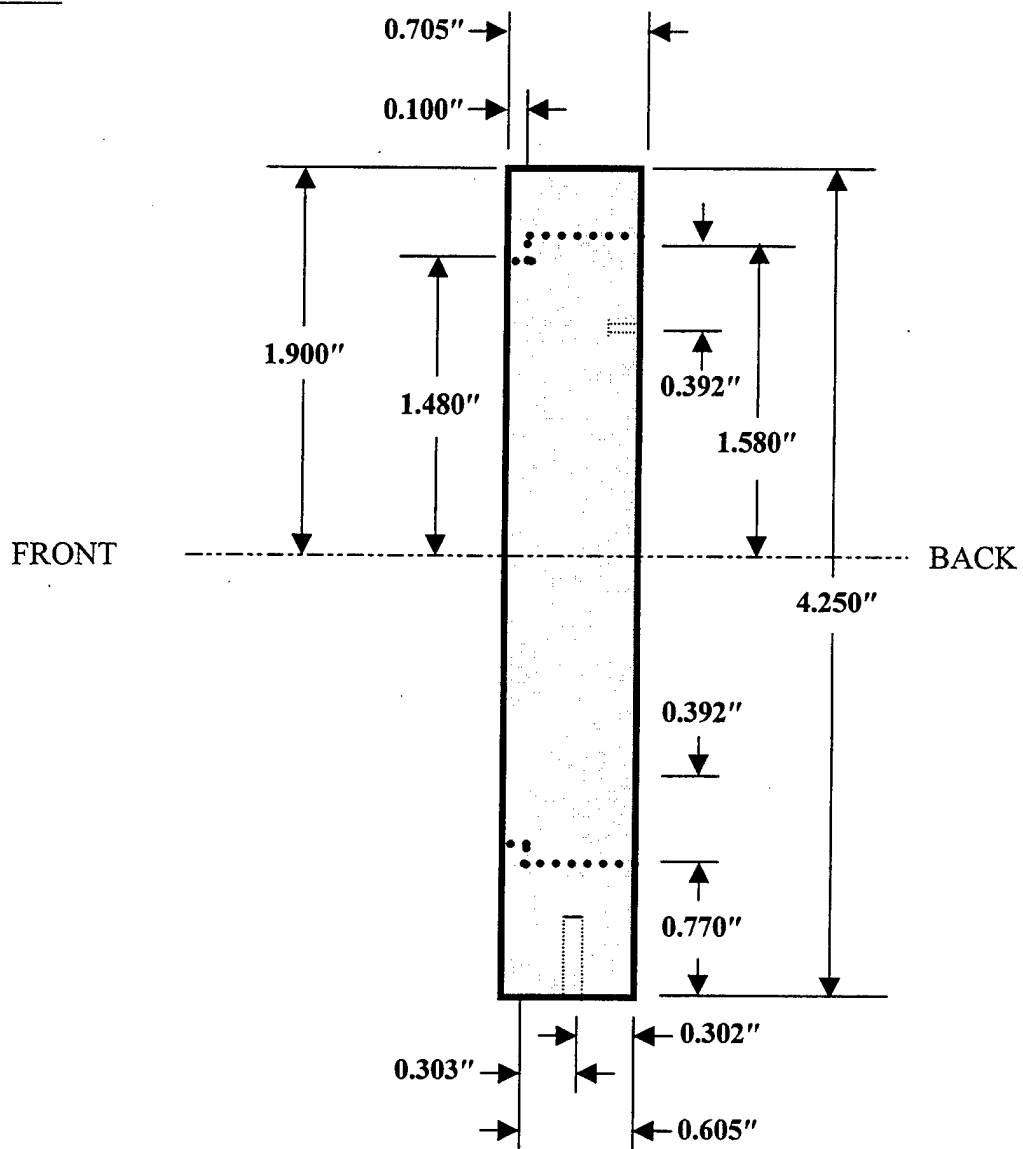
- Grating Mount and Spacer
- Mirror Spacers
- Rotator Plate Spacer
- Slit Mounts
- Grating Drive System
 - Motor Mount
 - Grating Drive (Gear Box)

DRAWING FOR DIFFRACTION GRATING MOUNT

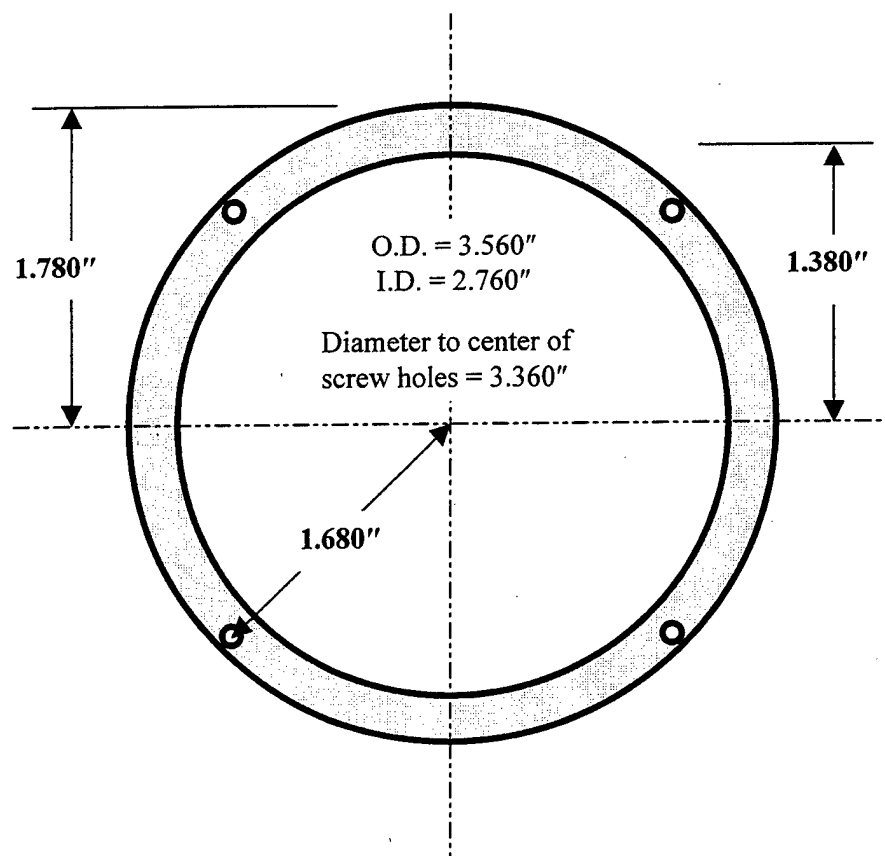
PART ONE: Diffraction grating mount with four small threaded screw holes, 0.250" deep around the perimeter (size 4-40 screws) for a washer type backing and three threaded holes through the bottom 0.500" deep (for size 8-32 screws).



SIDE VIEW:



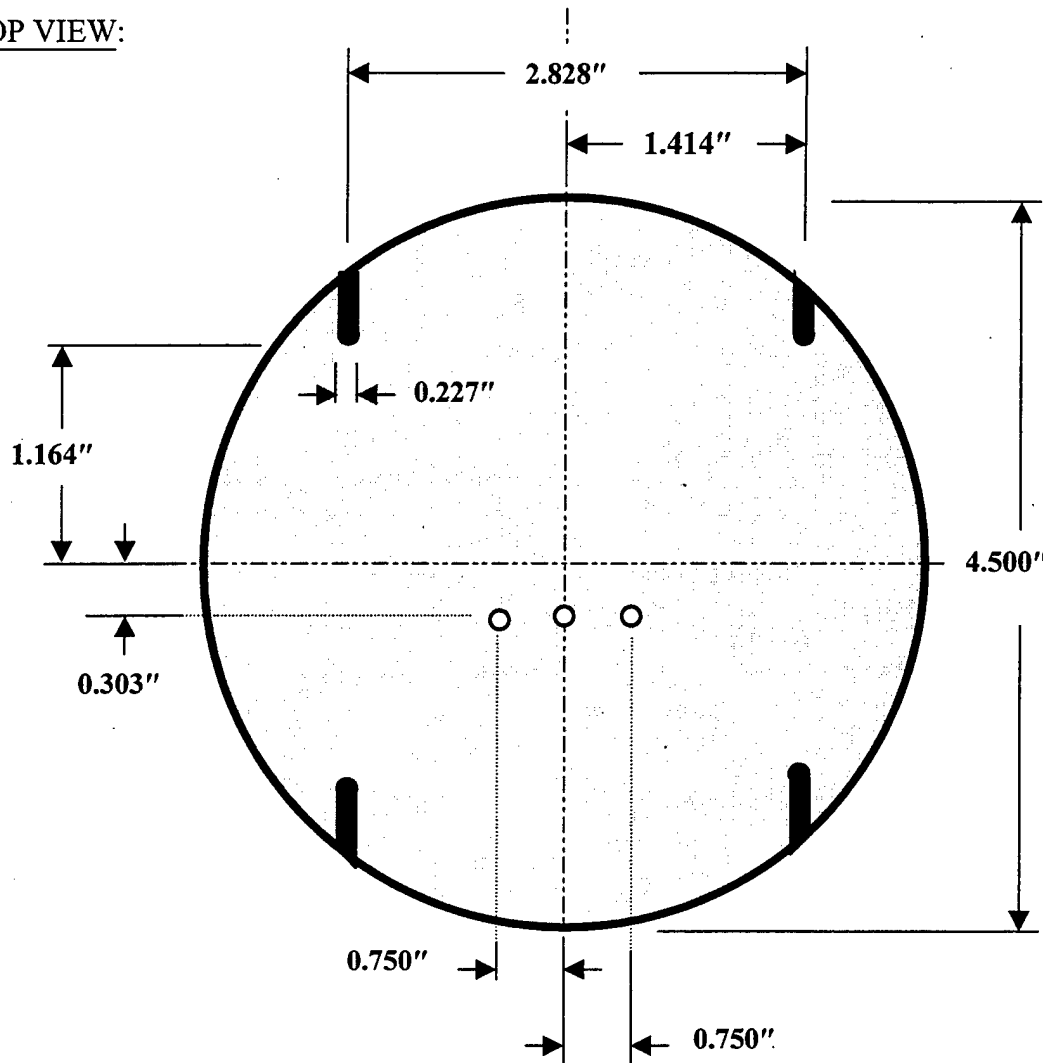
PART TWO: Washer type, compression backing 0.100" thick with 4 evenly spaced through holes for size 4-40 screws.



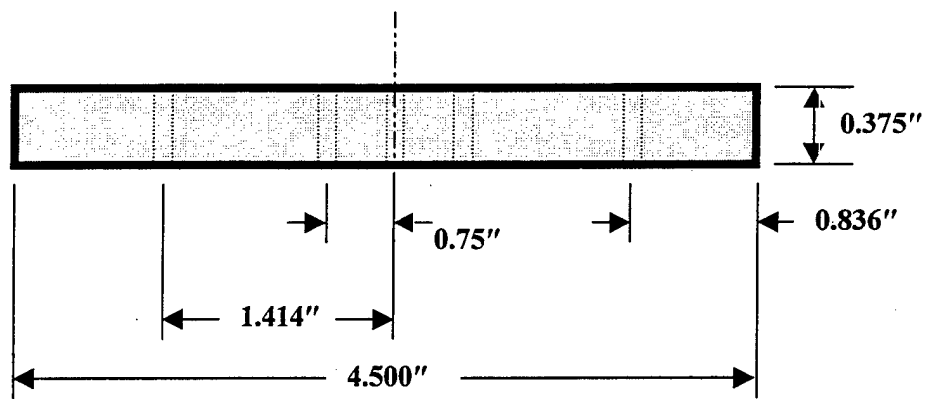
DRAWING FOR DIFFRACTION GRATING SPACER

PART 2: A 0.375" thick, 4.5" diameter circular aluminum spacer with four slots 0.227" in diameter, unthreaded, counter bored 0.328" diameter and 0.200" deep; and 3 threaded 8-32 holes near the center.

TOP VIEW:



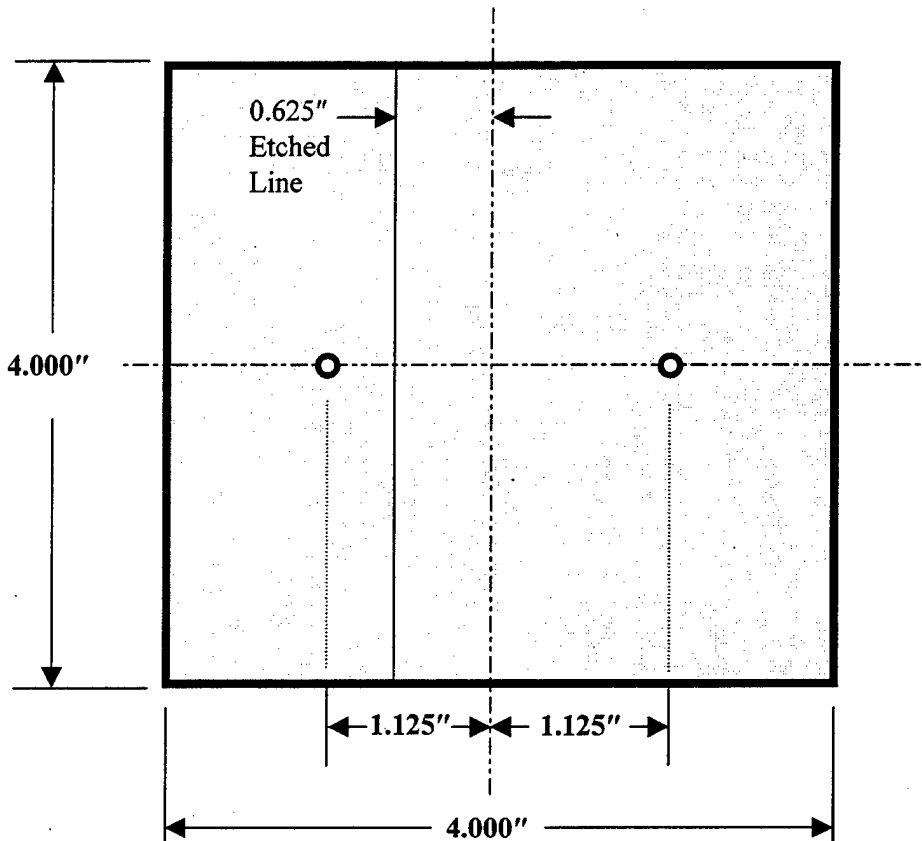
SIDE VIEW:



DRAWING FOR MIRROR MOUNT SPACERS

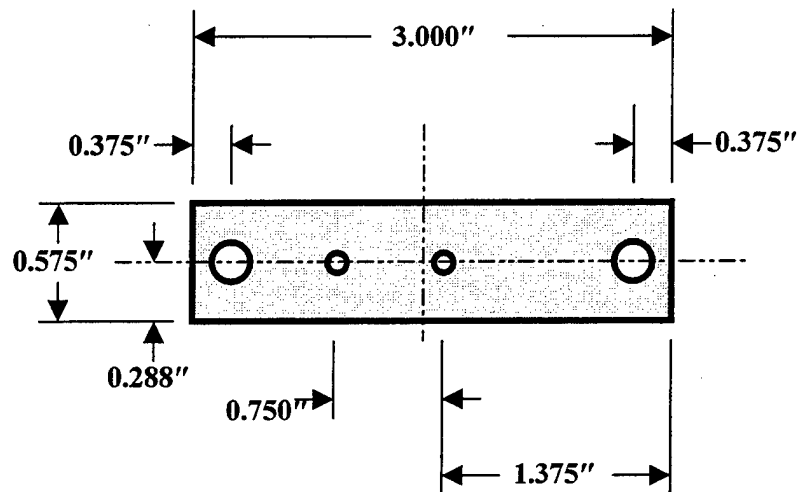
PART ONE: Bottom plate, 4" x 4", and 0.500" thick with 2 threaded holes (for size 8-32 screws) through the plate. Also, an "etched line" at 0.625" off center. (Need four of these)

TOP VIEW:

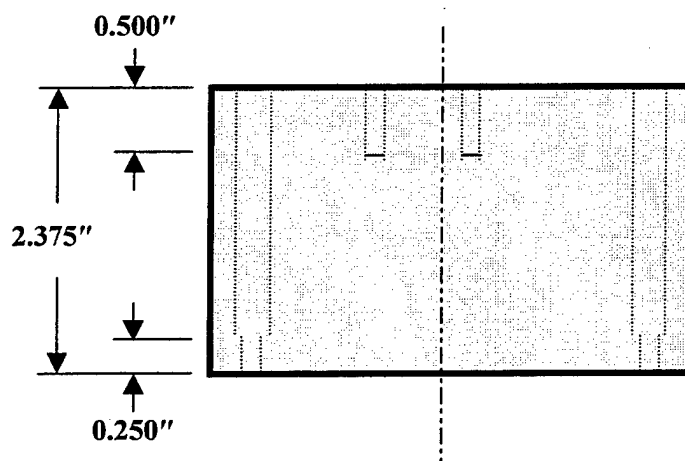


PART TWO: Spacer, 0.575" x 3.0", and 2.375" thick with 2 counter bored through holes (for size 8-32 screws), and two 0.5" deep threaded holes (for size 8-32 screws.) (Need four of these)

TOP VIEW:



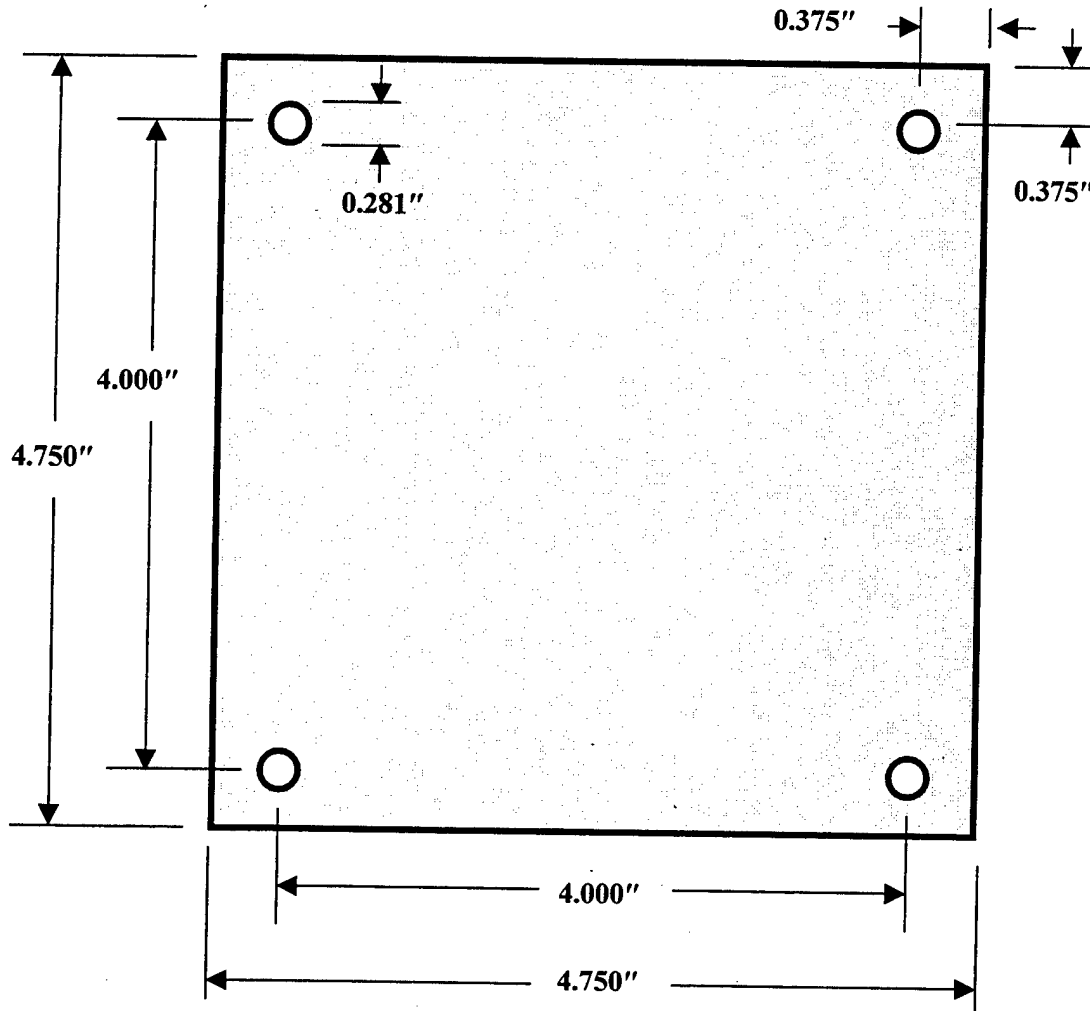
SIDE VIEW:



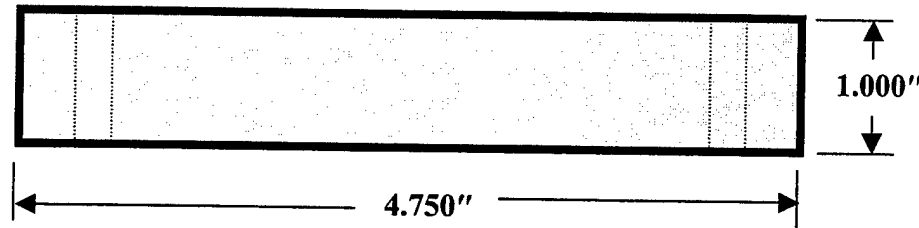
DRAWING FOR SLIT MOUNT

PART 1: A 1.0" thick, 4.75" x 4.75" square aluminum spacer with an unthreaded hole at each corner.

TOP VIEW:



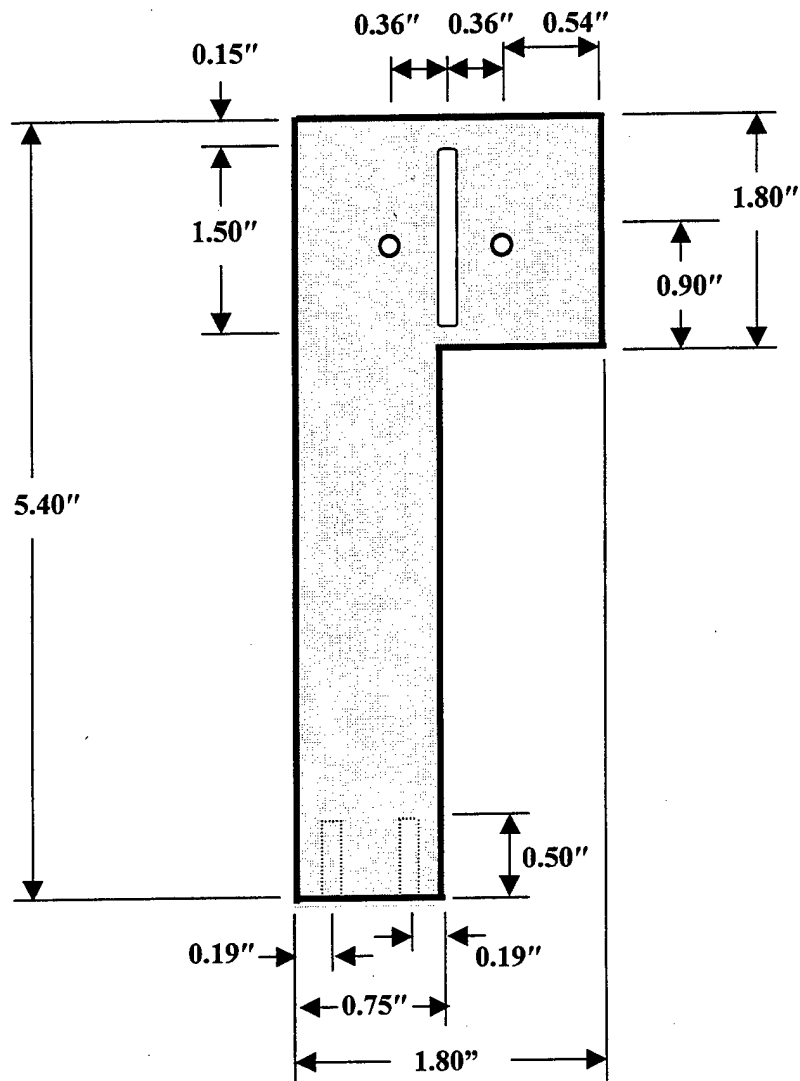
SIDE VIEW:



DRAWING FOR SLIT MOUNT

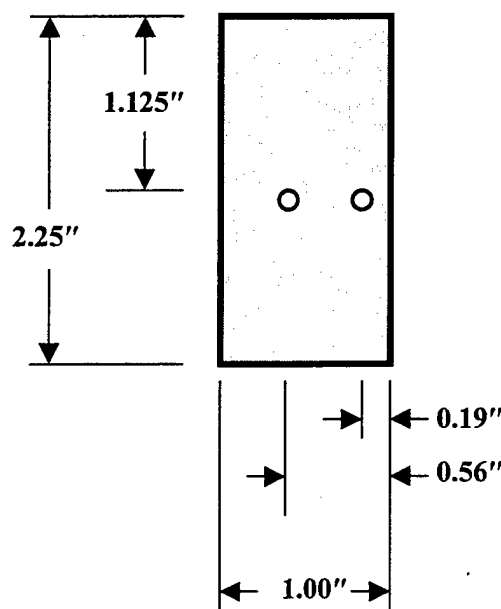
PART ONE: Slit support arm 0.25" thick with a 0.125" x 1.5"slit, two 2x56 threaded through holes and two 8x32 threaded holes 0.5" deep. (Need two of these)

FRONT VIEW:

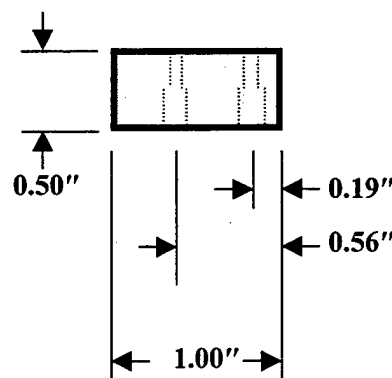


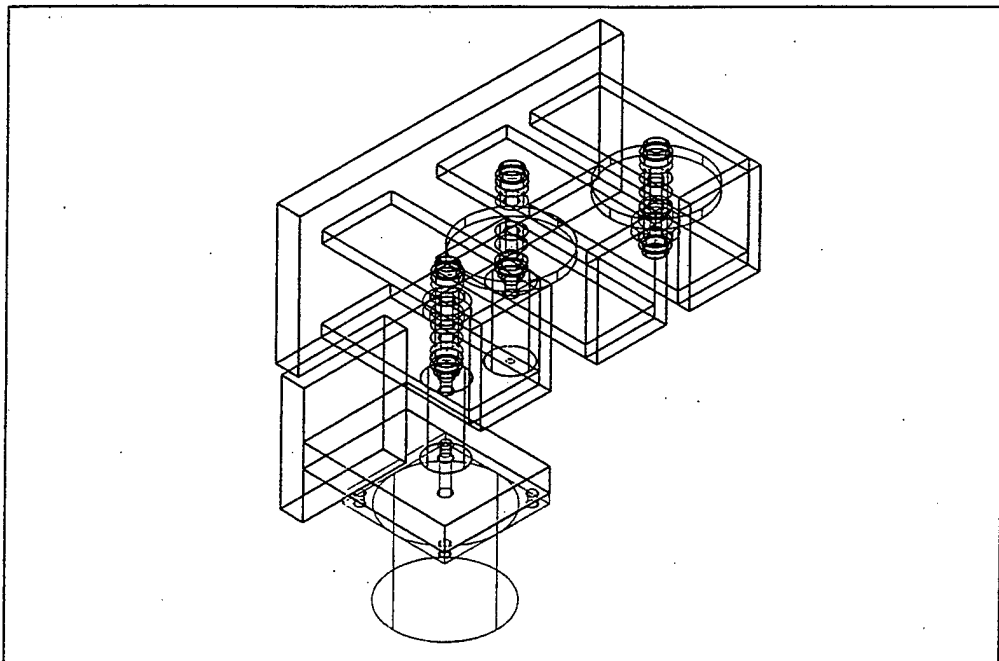
PART TWO: Base plate 0.5" thick, 2.25" long and 1.0" wide with two 8x32 counter bored through holes (counter bored 0.25" deep). (Need two of these)

TOP VIEW:

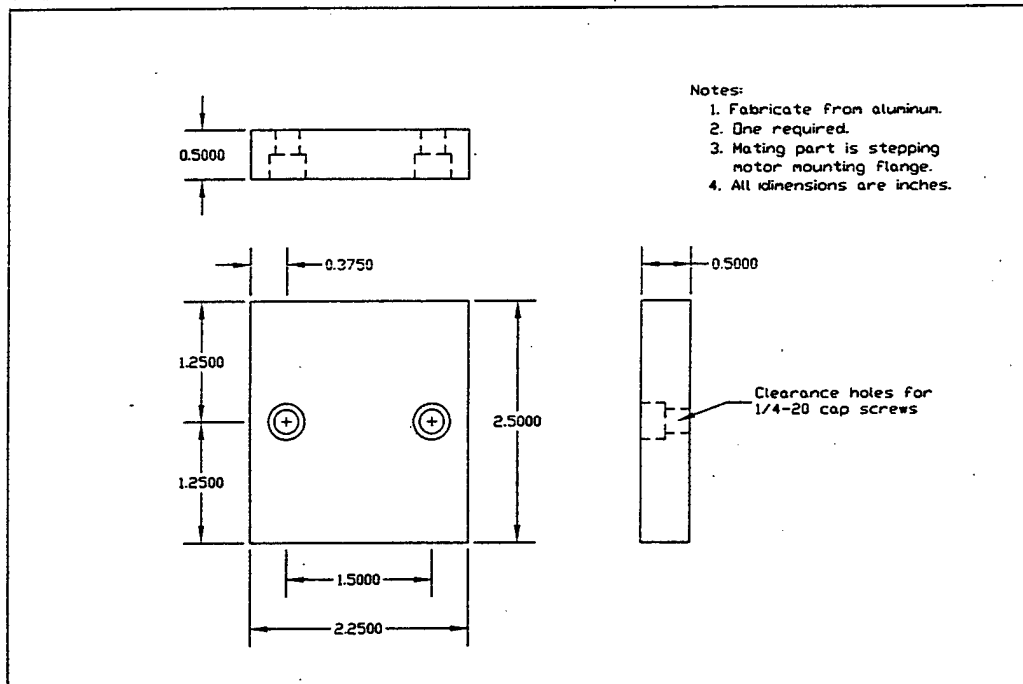


SIDE VIEW:

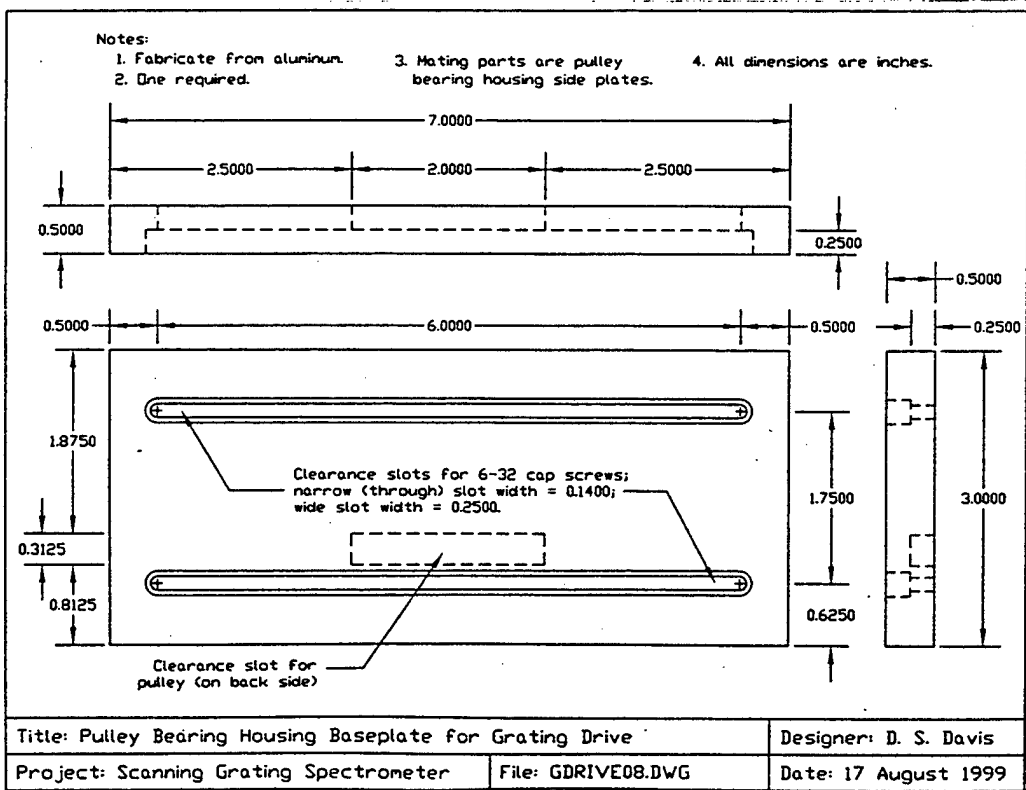
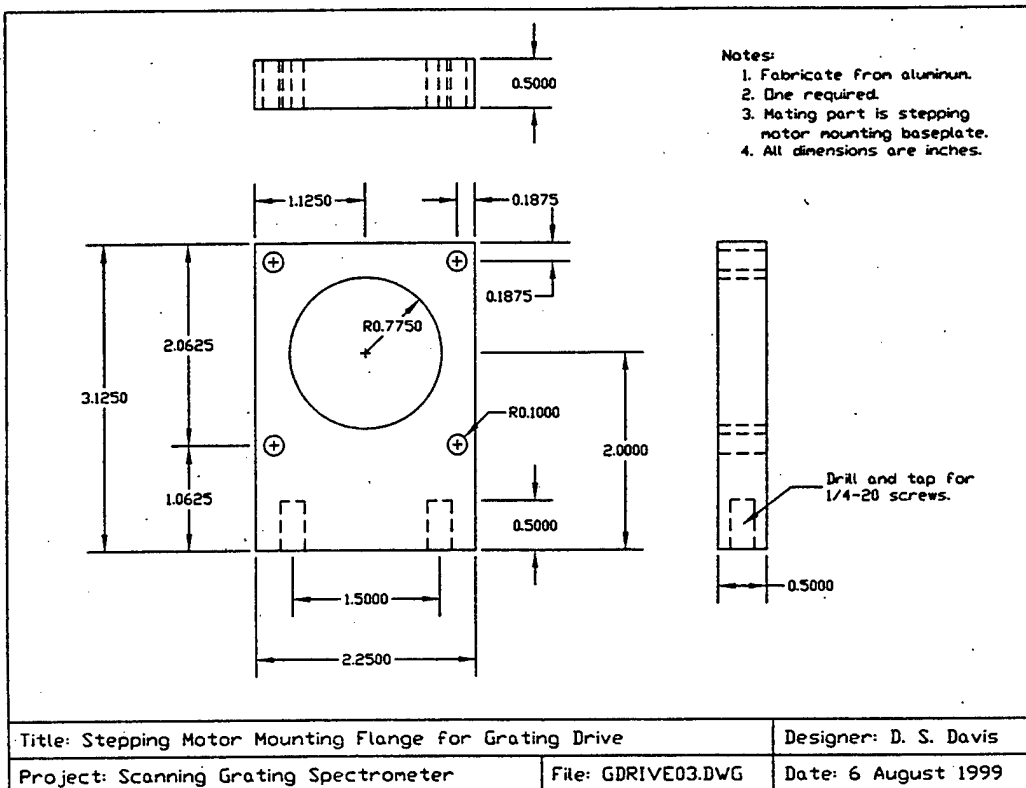


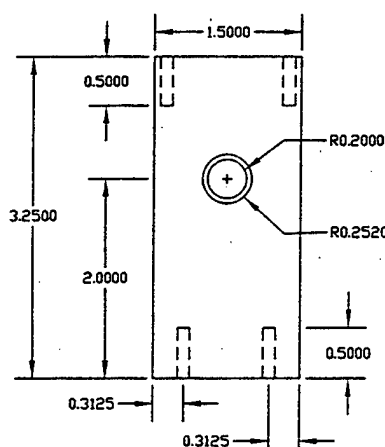
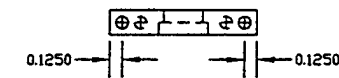


Title: Wire Frame Diagram of Grating Drive System	Designer: D. S. Davis
Project: Scanning Grating Spectrometer	File: GDRIVE02.DWG Date: 2 August 1999



Title: Stepping Motor Mounting Baseplate for Grating Drive	Designer: D. S. Davis
Project: Scanning Grating Spectrometer	File: GDRIVE04.DWG Date: 6 August 1999





Notes:

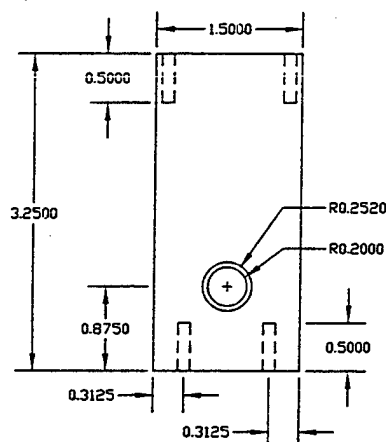
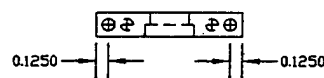
1. Fabricate from aluminum.
2. Four required.
3. Mating parts are pulley bearing housing top plates and pulley bearing housing baseplate.
4. All dimensions are inches.

Drill and tap for 6-32 screws.

Depth of offset = 0.1250

Drill and tap for 6-32 screws.

Title: Outer Pulley Bearing Housing Side Plate for Grating Drive	Designer: D. S. Davis
Project: Scanning Grating Spectrometer	File: GDRIVE06.DWG Date: 9 August 1999



Notes:

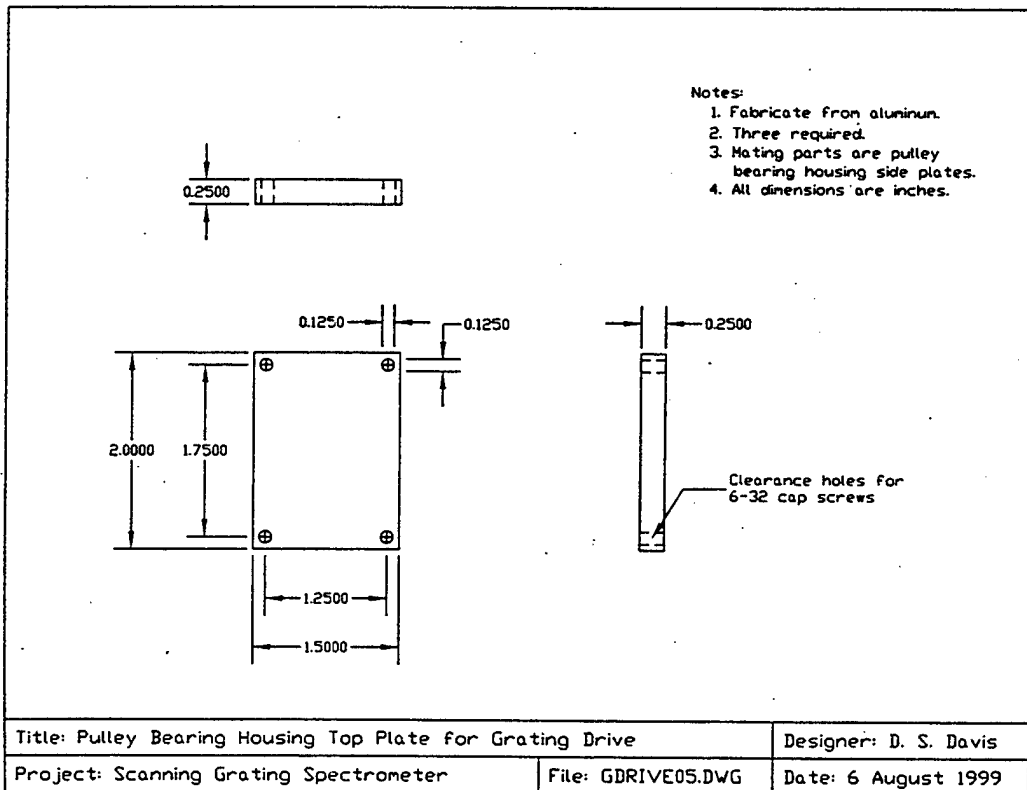
1. Fabricate from aluminum.
2. Two required.
3. Mating parts are pulley bearing housing top plates and pulley bearing housing baseplate.
4. All dimensions are inches.

Drill and tap for 6-32 screws.

Depth of offset = 0.1250

Drill and tap for 6-32 screws.

Title: Center Pulley Bearing Housing Side Plate for Grating Drive	Designer: D. S. Davis
Project: Scanning Grating Spectrometer	File: GDRIVE07.DWG Date: 9 August 1999



THIS PAGE INTENTIONALLY LEFT BLANK

APPENDIX B. MOTOR CONTROL COMPUTER PROGRAM

Microsoft Visual Basic 5.0 computer program

for spectrometer motor control.

'Program to control spectrometer motor via a computer screen
'user interface. Program has following motor control options:
'Start, Stop, Direction, Faster, Slower, Mark home position, and
'Return to home position.

'Author: James Hassett
'Date: June, 1999

'Version 4

Option Explicit

Dim velocity As String
Dim data As String
Dim direction As String

Private Sub cmdFaster_Click()
velocity = velocity + 0.5
data = "VC" + velocity
Transmit_Data (data)

End Sub

Private Sub cmdGohome_Click()
Dim distance As String
MSComm1.Output = "1PR" + vbCrLf
MSComm1.Output = "1PR sent"
Select Case MSComm1.CommEvent
Case comEvReceive
distance = MSComm1.Input
distance = Right(distance, 12)
If Left(distance, 1) <> "-" Then
direction = "-"
Else
direction = "+"
End If
distance = Right(distance, 10)
End Select
data = "LD3 ST0 MN A.5 V2.5 D" + distance + " H" + direction + " G "
MSComm1.Output = data + vbCrLf
data = "ST1"
MSComm1.Output = data + vbCrLf
MSComm1.PortOpen = False
data = ""
End Sub

Private Sub cmdSet_Click()
data = "PZ"
Transmit_Data (data)
End Sub

Private Sub cmdSlower_Click()
If velocity < 0.2 Then
data = "K"

```

        Transmit_Data (data)
        Data = "ST1"
        Transmit_Data (data)
    Else
        velocity = velocity - 0.2
        data = "VC" + velocity
        Transmit_Data (data)
    End If
End If

Private Sub cmdStart_Click()
    velocity = 0.5
    data = " LD3 ST0 MC A.5 V" + velocity + " H" + direction + " G "
    Transmit_Data (data)
End Sub

Private Sub cmdStop_Click()
    data = "K"
    Transmit_Data (data)
    data = "ST1"
    Transmit_Data (data)
End Sub

Private Sub optCCW_Click()
    direction = "-"
End Sub

Private Sub optCW_Click()
    direction = "+"
End Sub

Private Sub Form_Load()
    'Initialize the Comm Control to Comm1
    MSComm1.CommPort = 1
    MSComm1.Settings = "9600,N,8,1"
    Debug.Print "-----"

    'Comm event will be triggered when a single character is received.
    MSComm1.Rthreshold = 19
    MSComm1.Sthreshold = 1
End Sub

Public Function Transmit_Data (data As String)
    MSComm1.PortOpen = True
    MSComm1.Output = data + vbCrLf
    MSComm1.PortOpen = False
    data = ""
End Function

```

THIS PAGE INTENTIONALLY LEFT BLANK

APPENDIX C. TABLE OF TENTATIVE IRON LINE IDENTIFICATIONS

Table summarizes the spectrometer data and its tentative iron line identifications using published literature.

Tentative Line Identifications for Fe Hollow Cathode

Spectrum File Line Sample #	Relative Intensity	Calculated Wavelength (Angstroms)			Line Identification
		1 st Order	2 nd Order	3 rd Order	
444	0.4	8864	4432	2955	4430.62 4433.22
478	0.2	8849	4424	2950	4422.57
545	0.9	8818	4409	2939	4404.75 4407.71
570	1.2	8807	4403	2936	4401.30
707	4.6	8744	4372	2915	4375.93
905	1.2	8652	4326	2884	4325.76 4327.10
956	4.3	8629	4314	2876	4315.09
998	2.0	8609	4305	2870	4307.90
1001	1.8	8607	4304	2869	4305.45
1091	1.8	8566	4283	2855	4285.44
1299	4.4	8470	4235	2823	4235.94
1470	1.9	8390	4195	2797	4195.34 4194.24
1558	10.2	8349	4174	2783	4174.91 4176.57 4177.60
1716	2.2	8274	4137	2758	4137.00
1801	0.2	8234	4117	2745	4118.77 Co I?
1892	0.2	8191	4096	2730	4095.97 4098.19
1907	0.2	8184	4092	2728	4092.39 Co I?
2022	1.0	8130	4065	2710	4063.60 4066.98 4067.98
2056	0.2	8114	4057	2705	4058.23
2123	0.8	8082	4041	2694	4045.82
2392	0.8	7954	3977	2651	3977.75
3211	2.4	7560	3780	2520	3779.45
3225	5.5	7553	3777	2517	3775.72 Ti I?
3310	6.0	7512	3756	2504	3758.23
3339	0.5	7498	3749		3749.49
3400	15.0	7468	3734		3734.87 3737.13
3760	16.5	7293	3646		3647.85 7293.07
3896	16.0	7226	3613		3610.46 Ni I?
4131	1.5	7110	3555		3556.88

Tentative Line Identifications for Fe Hallow Cathode

Spectrum File Line Sample #	Relative Intensity	Calculated Wavelength (Angstroms)			Line Identification
		1 st Order	2 nd Order	3 rd Order	
4189	16.5	7082	3541		3540.12 3541.09 3542.08
4205	8.0	7074	3537		3536.56
4403	17.0	6976	3488		3490.57
4789	15.5	6784	3392		3392.65
4859	16.5	6749	3375		3370.78 3378.68 3380.11
4998	16.5	6680	3340		
5118	16.0	6620	3310		3310.34
5165	16.5	6596	3298		3298.13
5364	16.5	6496	3248		3245.98 3248.21 3251.23
5403	16.0	6476	3238		3234.62 3236.22 3239.44
5500	16.0	6428	3214		3214.04 3214.40
5560	13.5	6397	3199		3196.93 3199.52 3200.47
5637	15.5	6358	3179		3178.01 3180.76
5736	14.5	6308	3154		3151.35 3153.21 3156.27 3157.04 3157.89
5842	13.5	6255	3127		3125.65 3126.17 3129.34
5881	15.5	6235	3117		3116.63?
5910	1.5	6220	3110		6219.29
5969	15.0	6190	3095		3091.58
6009	14.5	6170	3085		3083.74
6086	6.5	6131	3065		3067.24
6177	5.5	6084	3042		3042.67 3047.61

Tentative Line Identifications for Fe Hallow Cathode

Spectrum File Line Sample #	Relative Intensity	Calculated Wavelength (Angstroms)			Line Identification
		1 st Order	2 nd Order	3 rd Order	
6230	13.0	6057	3029		3020.64 3025.64 3025.84 3026.46 3030.15 3031.21 3031.64
6299	0.5	6022	3011		6021.83
6305	0.5	6019	3010		6013.50 6016.65
6339	8.0	6002	3001		2999.51 3000.45 3000.95
6390	16.0	5976	2988		2983.57 2984.83 2986.46 2987.29
6446	0.7	5947	2974		2970.10 2972.28 2973.13 2973.13 2973.24 2976.13
6545	0.8	5897	2948		2947.88 2950.24 2953.94
6631	0.2	5852	2926		
6709	0.2	5812	2906		
6891	0.2	5719	2859		
6907	0.2	5711	2855		5709.39
7229	0.2	5544	2772		2772.12
7249	0.4	5534	2767		5530.77 Co?
7361	0.3	5476	2738		5473.72 5474.92
7385	0.3	5464	2732		5463.28
8114	0.3	5084	2542		2535.61
8758	0.3	4747			4749.68 Co?
8967	0.3	4636			4637.52
9650	0.2	4275			4274.81 Cr?
10075	0.3	4048			4045.82
10359	0.2	3897			3895.66 3897.89 3899.71
11604	0.2	3227			

LIST OF REFERENCES

1. Bass, M., *Handbook of Optics*, Vol. 2, pp. 5.8-5.13, McGraw-Hill, Inc., 1995.
2. Hecht, E., *Optics*, 3rd ed., pp. 265-266, Addison Wesley Longman, Inc., 1998.
3. Hecht, E., *Optics*, 3rd ed., p. 465, Addison Wesley Longman, Inc., 1998.
4. Hecht, E., *Optics*, 3rd ed., p. 468, figure 10.36, Addison Wesley Longman, Inc., 1998.
5. Maystre, D., *Rigorous Vector Theories of Diffraction Gratings*, Elsevier Science Publishers B. V., 1984.
6. Hecht, E., *Optics*, 3rd ed., p. 469, figure 10.38, Addison Wesley Longman, Inc., 1998.
7. Hecht, E., *Optics*, 3rd ed., pp. 469-471, Addison Wesley Longman, Inc., 1998.
8. Sinclair Optics, Inc., *Download OSLO LT*, [<http://www.sinopt.com/dloadlt.htm>], October 1998.
9. Barnhart, D., *Optica – Designing Optics with Mathematica*, 1st ed., Wolfram Research, Inc., 1995.
10. Halliday, D., Resnick, R., Walker, J., *Fundamentals of Physics Extended*, 5th ed., pp. 931-937, John Wiley and Sons Inc., 1997.
11. Compumotor Division of Parker Hannifin, *AX Drive Operator's Manual*, 1988.
12. Aitken, P., *Visual Basic 5 Programming Explorer*, The Coriolis Group, Inc., 1997.
13. New Focus, Inc., *Models 2151 & 5153 Visible & IR Femtowatt Photoreceivers User's Manual*.
14. Horowitz, P., Hill, W., *The Art of Electronics*, 2nd ed., p. 1032, figure 15.38, Cambridge University Press, 1989.
15. Hewlett Packard, *HP 34970A Data Acquisition/Switch Unit User's Guide*, 2nd ed., 1997.
16. U.S. Department of Commerce, National Bureau of Standards, *Tables of Spectral-Line Intensities Part I – Arranged by Elements*, 2nd ed., pp. 121-127, U.S. Government Printing Office, Washington, D.C., 1975.

17. Microsoft Corp., *Getting Results with Microsoft Office 97*, pp. 591-601, 1996.
18. U.S. Department of Commerce, National Bureau of Standards, *Tables of Spectral-Line Intensities Part I – Arranged by Elements*, 2nd ed., pp. 121-127, U.S. Government Printing Office, Washington, D.C., 1975.

INITIAL DISTRIBUTION LIST

1. Defense Technical Information Center 2
8725 John J. Kingman Rd., STE 0944
Ft. Belvoir, Virginia 22060-6218
2. Dudley Knox Library 2
Naval Postgraduate School
411 Dyer Rd.
Monterey, California 93943-5101
3. Curriculum Officer, Code 34 1
Engineering and Technology
Naval Postgraduate School
Monterey, California 93943-5101
4. Chairman, Code PH 1
Department of Physics
Naval Postgraduate School
Monterey, California 93943-5101
5. Professor Scott Davis, Code PH/Ds 2
Department of Physics
Naval Postgraduate School
Monterey, California 93943-5101
6. Professor Andres Larraza, Code PH/La 1
Department of Physics
Naval Postgraduate School
Monterey, California 93943-5101
7. Mr. James E. Hassett Jr. 3
29 Memorial Drive
Gowanda, New York 14070